WATER RESOURCES
research center

PUBLICATION NO. 109

MODEL OF POROSITY DEVELOPMENT IN A
COASTAL CARBONATE AQUIFER SYSTEM

BY

Anthony F. Randazzo

UNIVERSITY OF FLORIDA
GAINESVILLE, FLORIDA   32611

UNIVERSITY OF FLORIDA

MODEL OF POROSITY DEVELOPMENT IN A

COASTAL CARBONATE AQUIFER SYSTEM

by

Anthony F. Randazzo

Department of Geology
University of Florida
Gainesville, Florida   32611

TABLE OF CONTENTS

ABSTRACT

A conceptual model of the evolution of porosity through time and space was formulated for carbonate aquifer rocks in coastal regions of the Southwest Florida Water Management District. This model focused on an understanding and recognition of primary and secondary noncavernous porosity development in five cores from this area. Water/rock interactions and geologic processes were evaluated in terms of the sequential formation of the porosity observed today. Micritization, compaction, dissolution, cementation and replacement (dolomitization, calcification, and silicification) were related to porosity types, abundances, and occurrences.

Positive correlations between relatively high permeability and porosity, as well as relatively low permeability and porosity, could be made for some sequences. Other rock sequences showed no correlation between these parameters suggesting cavernous conditions or varying degrees of diagenetic alteration in dolomitic horizons. Groundwater flow paths reflect the high porosity/permeability relationship. Stratigraphic considerations suggest that certain intervals of the Suwannee, Ocala, and Avon Park units were fine-grained shallow water deposits which were subjected to more intensive diagenesis and porosity development.

Lithofacies relationships reveal that packstones and grainstones produce more interparticle and moldic porosity,

1

whereas carbonate mudstones and wackestones produce more vug porosity. Dolomitized sections of rock display more intercrystal, intracrystal, and vug porosity. Trace element concentrations (sodium and strontium) and stable isotope data (carbon and oxygen) for dolomite mimic the porosity type/distribution relationships of dolomite occurrences. Generally, these geochemical parameters are affected by the same diagenetic processes responsible for dolomitization.

Present day porosity is a reflection of original rock types, including environments of deposition, and the diagenetic processes which have been operating for more than 30 million years. Calcite and dolomite dissolution and the creation of different types and abundances of porosity have been complexed by varying hydrologic regimes including multiple migrations of the saltwater/freshwater mixing zone. The dynamics of these geochemically reactive aqueous systems has also produced numerous phases of porosity destruction through cementation and dolomitization.

INTRODUCTION

Porosity is among the most important parameters used in hydrologic studies. Groundwater quality and flow models are dependent upon accurate quantitative information concerning the percentage, size, type, and distribution of pore spaces in aquifer rocks. Assumptions are often made about these aspects of porosity because data are lacking. Such assumptions can affect the accuracy of the predictive output of the models.

This study is an attempt to formulate a conceptual model of the evolution of porosity through time and space. Parts of the coastal area of the Southwest Florida Water Management District (SWFWMD) were the geographical focus of the research (Fig. 1). A mineralogical model, developed for this region (Randazzo, 1983) was integrated with the porosity model in order to define water/rock interactions as they apply to porosity creation and destruction.

This project attempts to fill an important gap in available knowledge on the specific reasons for porosity development and its occurrence. How is porosity of the carbonate rocks related to groundwater flow paths and areas of recharge and discharge? How is porosity related to stratigraphic horizon? How is porosity related to the distribution of various lithologies? How is porosity related to the distribution of trace elements in carbonate rocks of the aquifer? Where is porosity forming today, in what manner, and under what geochemical conditions? These

3
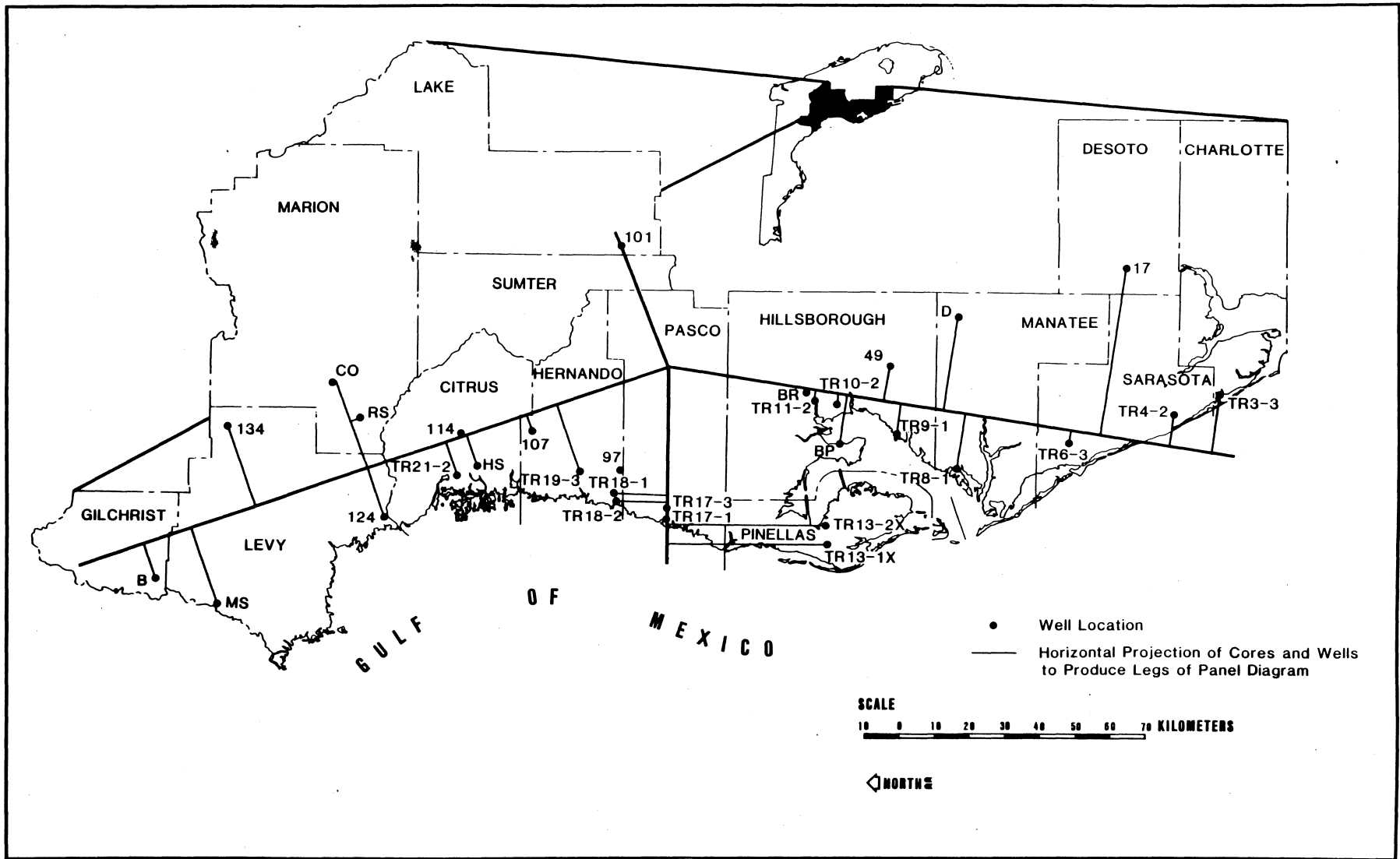
Figure 1. Location of cores and wells in study area. Connected lines are keyed to panel diagrams (Figs. 23, 24, 30, 31 and 32).

questions were addressed through the formulation of a porosity model for the coastal carbonate aquifer system.

Miller (1986) has integrated the most recent stratigraphic overview with a regional hydrogeologic framework for rocks of the Floridan Aquifer System. The Avon Park Formation, the Ocala Limestone and the Suwannee Limestone are the principal units comprising the upper aquifer system, the principal focus of this study. These formations have experienced extensive diagenetic changes, including dolomitization and dissolution, which are of particular significance in the porosity changes of the aquifer. The hydrogeological importance of the Upper Floridan Aquifer System is its high permeability, thickness, and widespread distribution. High yields of potable groundwater are realized by this system.

Cavernous and Non-cavernous types of porosity affect regional development of carbonate aquifer systems and the geologic history of an area. This study researched the non-cavernous porosity aspects of the coastal aquifer. However, certain considerations of the cavernous porosity have been addressed through publication review and the data of other workers.

METHODS OF STUDY

The area selected for study was the coastal groundwater system in the Southwest Florida Water Management District (SWFWMD). Hernando, Pasco, and Pinellas Counties were the principal region of focus, although cores from Levy,

5

Hillsborough, Citrus, and Charlotte counties were also included. Rock core and water chemistry data associated with the Regional Observatory and Monitoring-Well Program (ROMP) of SWFWMD were utilized for this study. Figure 1 depicts the location of the cores used. More than 500 rock samples were examined from these cores. Parts of all samples were powdered for X-ray diffraction analyses to determine qualitative mineralogy. Thin sections were prepared for petrographic study. Some thin sections were polished for microprobe analyses. Modal analysis was conducted on all thin sections to determine quantitative distribution of rock constituents and types of visible porosity. A JEOL Superprobe 733 was used to determine Ca/Mg ratios of dolomite crystals.

Numerous pore spaces in the rock core samples were examined with a ISI-DS 130 dual stage scanning electron microscope (SEM). Dissolution effects and general crystal morphology were identified for different pore types. Specific compositional analyses were also completed using an ORTEC energy dispersive X-ray fluorescence attachment to the SEM.

Geochemical analyses of rock samples consisted of determining concentrations of the trace elements Na and Sr using a Perkin-Elmer model 403 atomic absorption spectrophotometer. Carbon and oxygen isotopic compositions were determined for selected dolomite samples. Analyses were carried out at the Geological Institute, ETH Zentrum,

Zurich, Switzerland with a VG Micromass 903 mass spectrometer.

Water data routinely collected by SWFWMD include temperature, specific conductance, pH, hardness, alkalinity, bicarbonate, total dissolved solids, Ca^{+2}, Mg^{+2}, K^+, Na^+, Cl^-, F^-, and $SO4$. These data were utilized in determining the stability of carbonate minerals in the rock cores. The FORTRAN program WATEQF (Plummer et al., 1976) was used to calculate these stabilities. The program output consists of the ion activity, the equilibrium constant, and the saturation index for each carbonate mineral species.

Selected core samples from various locations in five cores were analyzed for permeability by Core Laboratories of Dallas, Texas. Results are reported in millidarcies (md).

NON-CAVERNOUS POROSITY

Porosity is the percentage of open (pore) spaces in a rock. Primary porosity is the original voids produced by the sedimentological arrangements of rock constituents (intraclasts, fossils, pelloids). All changes affecting the sediments (lithification, compaction, dissolution, diagenesis and tectonism) result in an enhancement or destruction of original porosity and the formation of secondary porosity. This evolutionary development can be highly variable and ultimately results in large scale cavernous spaces. The distinction has not been precisely defined but, as used in this study, an opening of 10 cm is used as the boundary. This size limit was found to be

workable as a means of characterizing pore character. The terminology and conceptual scheme of Choquette and Pray (1970) was used in this study. Selective or non-selective porosity development is well articulated by Choquette and Pray (1970). Differential dissolution, early and late stage cementation, and other diagenetic processes can account for the percentage, type, and distribution of the resulting porosity.

Initial porosity in carbonate sediments is generally estimated to be 40-70% of the total volume (Choquette and Pray, 1970). It may ultimately be reduced to one or two percent. Fine-grained carbonate sediments (mudstones) possess the highest primary porosity while lower porosity occurs in carbonate grainstones (Scholle, 1979).

Secondary porosity results from sediment compaction, dissolution, mineral inversion and replacement, pore-filling cementation, and recrystallization. Inversion of original argonite to its polymorph calcite can result in a 15-20% decrease in porosity. Schmoker and Hester (1986) have related this mineralogical inversion phenomenon to the distribution of porosity in the Pleistocene Miami Limestone. Depth of burial and the factors operating under these conditions of overburden have also been related to porosity changes. In south Florida, carbonate porosity is half as much at depths of 1700 m than at the surface (Schmoker and Halley, 1982).

Replacement of calcite by dolomite can produce both increases and decreases in porosity, depending upon the manner and degree of replacement (Murray and Pray, 1965; Blatt et al., 1980; Schmoker et al., 1985). Dolomite has a 12% lower molar volume than calcite which could bring about a similar degree of porosity reduction (Bathurst, 1975; Morrow, 1982). However, calcite dissolution and replacement by dolomite may be a volumetric rather than a molar process, resulting in variations in the ultimate rock porosity.

Choquette and Pray (1970) indicated that moldic and vug porosity are the most common in limestone. Interparticle porosity is most abundant in calcareous grainstones. Intercrystalline and vuggy porosity types are characteristic of dolomite sequences. Results of visible porosity types and abundance are presented in Table 1.

Porosity types and abundances are related to the original depositional fabric and diagenetic history of the rocks. A general trend of decreasing porosity with depth is apparent in all cases. The collection of scanning electron photomicrographs included in this report (Figs. 2-17) reveal a number of pore-lining relationships. They illustrate an overwhelming presence of pore-filling calcite and dolomite crystals into previously dissolved areas of the rocks. In a few situations, these pore-filling crystals have themselves experienced partial dissolution.

Table 1. Visible Porosity - Types and Abundances

Core 13-2X

Pore Types and Percentages

Sample Number	Depth (m)	Moldic	Inter-Particle	Intra-Particle	Inter-Crystal	Vug	Other	Total Visible Porosity (%)
1	129.5	10.1	3.3	4.8		6.0		24.2
2	130.1	0.9		1.7		14.3	0.6	17.5
3	130.9	1.3	2.3	0.7				4.3
4	134.1	4.4	4.4	4.4		7.4		20.6
5	138.4		29	2.3				31.3
6	151.1		21.2	2.7		0.3		24.2
7	151.4	5.6		2.7		7.7	0.6	16.6
8	152.0					3.7		3.7
9	153.8					3.6	0.6	4.2
10	154.8				0.7		0.4	1.1
11	157.5	0.9	10.2	1.2				12.3
12	160.0	2.6	1.8	0.5		1.8		6.7
13	167.0	0.5	25.7	0.8				27.0
14	169.7		21.7	0.6				22.3
15	171.5		7.3			3.0		10.3
16	174.7	0.5	9.1	5.2		5.2		20.0
17	175.1		1.2	1.2		0.9		3.3
18	179.1	0.6	4.2	2.1		1.2		8.1
19	179.6	0.6	1.7	0.3		2.0	0.9	5.5
20	180.6	0.8	0.5	0.5		0.5		2.3
21	181.9	1.8		0.6		2.9		5.3
22	185.2	0.6		1.5		12.1		14.2
23	186.0					0.3	0.9	1.2
24	187.4	1.2		2.1		6.9		10.2
25	190.5			0.6		3.4		4.0
26	192.6	1.8	2.1	1.2		4.3		9.4
27	196.4	4.8		1.5		3.0		9.3
28	199.0	0.6	8.0			3.7		12.3
29	201.9	0.9	8.0	1.5		2.0		12.4
30	202.3	0.3			22.5	0.3		23.1
31	205.1	0.3	2.5	0.6	0.9	0.6		4.6

Core TR3-3

Sample Number	Depth (m)	Moldic	Inter-Particle	Intra-Particle	Inter-Crystal	Vug	Other	Total Visible Porosity (%)
1	274.6	1.9	16.8	1.2		1.9		21.8
2	274.9	5.2	9.7	1.2		3.6		19.7
3	276.2	1.2	2.0	0.9		1.2	0.6	5.9
4	276.7	0.6	6.9	2.1		1.2		11.8
5A	278.5					1.6	2.7	4.3
6	278.7		0.3	0.6		1.2		2.1
7	278.9	0.3	5.1	0.9		0.9		7.2
8	279.4		2.0	1.8		0.9		4.7
9	279.9				0.6	0.3		0.9
10	281.2				0.6	1.2		1.8
11	281.3				1.2	2.1		3.3
12	281.6					0.3		0.3

Table 1. (continued)

CORE ROMP 17

Sample Number	Depth (m)	Moldic	Inter-Particle	Intra-Particle	Inter-Crystal	Vug	Other	Total Visible Porosity (%)
1	243.5		1.5	1.2		1.2		3.9
2	243.9	0.5	3.1	0.3		0.8	0.3	5.0
3	245.7	0.6	0.9	0.3		0.3		2.1
5	246.9	0.6		0.3		0.9		1.8
6	247.7	0.3		0.6		1.3		2.2
7	248.7	1.1		1.1		3.3	0.3	5.8
9	249.5			0.3		5.2		5.5
10	249.8					5.9		5.9
11	249.9			0.4		2.8		3.2
12	250.1	0.3	0.3	0.3		2.5		3.4
13	251.6	2.2	2.2	1.3		1.9		7.6
14	252.5	0.9	1.2	0.3		0.3		2.7

CORE TR18-2

Sample Number	Depth (m)	Moldic	Inter-Particle	Intra-Particle	Inter-Crystal	Vug	Other	Total Visible Porosity (%)
1	151.8	3.3				1.0		4.3
3	153.6				14.1	1.9		16.0
5	156.1	11.7	0.3		1.7	0.7		14.4
8	160	2.3		1.0	5.2	0.7		9.2
9	162.5	1.0	4.0	1.3	1.7	1.0		9.0
14	169.2	5.9			1.6			7.5
15A	169.3	4.0			0.7	0.7		5.4
17	172.8	2.0		0.7	1.6	2.0	2.7	9.0
18B	174.8	5.0			6.3		4.0	15.3
21A	181	9.1			3.1	0.7		12.9
24	193.9	1.6			3.0	1.3	1.0	6.9
26	197.8	1.3			2.7	1.0		12.0
27	198.7	1.0			3.0			4.0
28	200.6	7.6	3.0	1.3	1.0	2.3		15.2
29	202.7	7.0			6.6	2.3		15.9
31	208.9	14.7			2.7	6.7		24.1
34	214.7	7.2			1.0	4.0		12.2
35	217.2	1.6	2.9	6.5	3.6	2.3	2.3	13.2
38	221.6	7.1	0.7	3.7		4.8	0.7	16.9
41	227.8	1.4			0.7	1.4		3.5
45B	231.6	0.6			0.3			0.9
47	234.4	6.7			0.3	4.6		11.6
53	245.1	6.0			1.6	5.4		13.0
55	248.1	2.7			4.0	2.7		9.4

Table 1. (continued)

CORE TR13-1X

Sample Number	Depth (m)	Moldic	Inter-Particle	Intra-Particle	Inter-Crystal	Vug	Other	Total Visible Porosity (%)
1	135	0.4				12.6		13.0
2	142	10	0.4			15.8		26.2
3	143	1.3				14.9		16.2
4	145	0.6				4.1		4.7
5	146					1.6		1.6
6	148	2.8				12.1		14.9
7	150	0.8			0.4	0.4		1.6
8	151	0.3			0.3	2.5		3.1
9	152	0.7			0.7	5.9		7.3
10	153	3.3				3.0		6.3
11	154	0.2	0.2			4.4		4.8
12	155	2.9	4.1	0.6		7.4		15.0
13	157	0.7				11.6		12.5
14	158	1.1				14.3		15.6
15	161	0.3				10.6		10.9
16	165	0.5				5.9		6.4
17	171	0.2				2.1		2.3
18	172	1.2				4.3		5.5
19	176	0.8				6.3		7.1
20	181	0.8				8.4		9.2
21	182	2.5				1.8	1.8	6.1
22	186					1.0		1.0
23	190	0.6		0.6		3.8		5.0
24	195	1.6	2.4	0.7		7.1		11.9
25	196	5.2	1.7	1.2		6.1		14.2
26	198		1.7			5.1		6.8
27	201	2.6	1.5			7.1		11.2
28	203	0.3	4.8			8.4		13.5
29	206	0.3	0.5			12.6		13.4
30	209	1.2	0.7			8.5		10.4
31	210	0.9				1.9		2.8
32	211	3.2				1.3		4.5
33	212					0.7		0.7
35	215	0.3				9.9		10.2
36	217					0.7		0.7
37	221	1.3			0.2	3.2		4.7
38	222					0.3		0.3
39	224		0.5			0.5		1.0
40	225					7.7		7.7
41	226					11.6		11.6
42	227	1.0		0.1	0.1	2.2		3.4
43	231					7.8		7.8
44	233					6.5		6.5
45	234	0.3	5.8			8.8		14.9
46	235		1.0			7.8		8.8
48	237					13.8	0.7	14.5
49	238	1.0			0.3	5.4	0.3	7.0
50	239	1.4			1.4	18.8		21.6
51	241				1.3	19.6		20.9
52	242					0.5	0.5	1.0
53	243				0.9	4.4	0.3	5.6
54	244				0.9	2.3		3.2
55	245					4.0		4.0
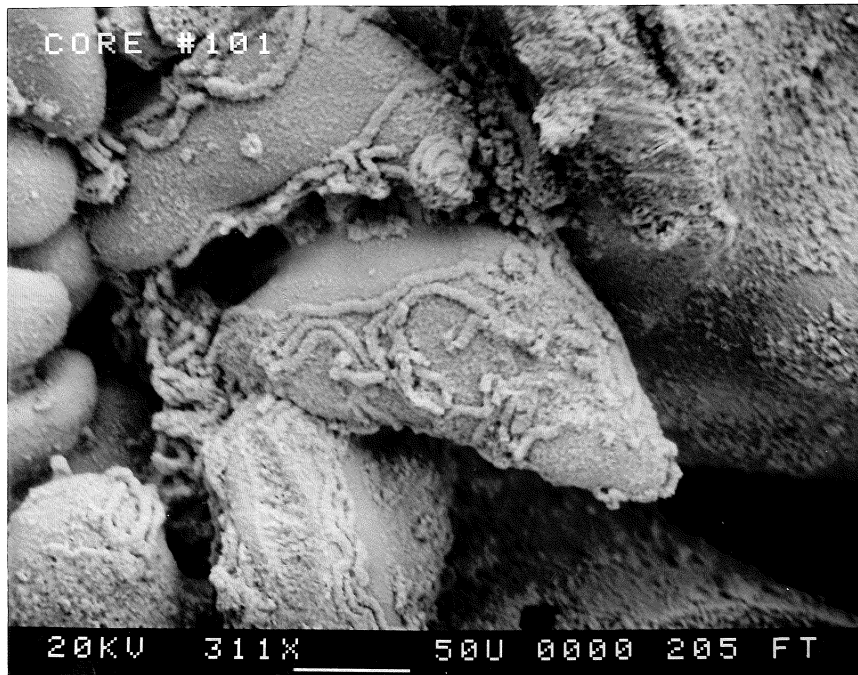
Figure 2. SEM photomicrograph of primary interparticle porosity among
skeletal grains (foraminifers); note trails left by boring algae
involved in grain micritization. Core 101, sample depth: 205 ft.
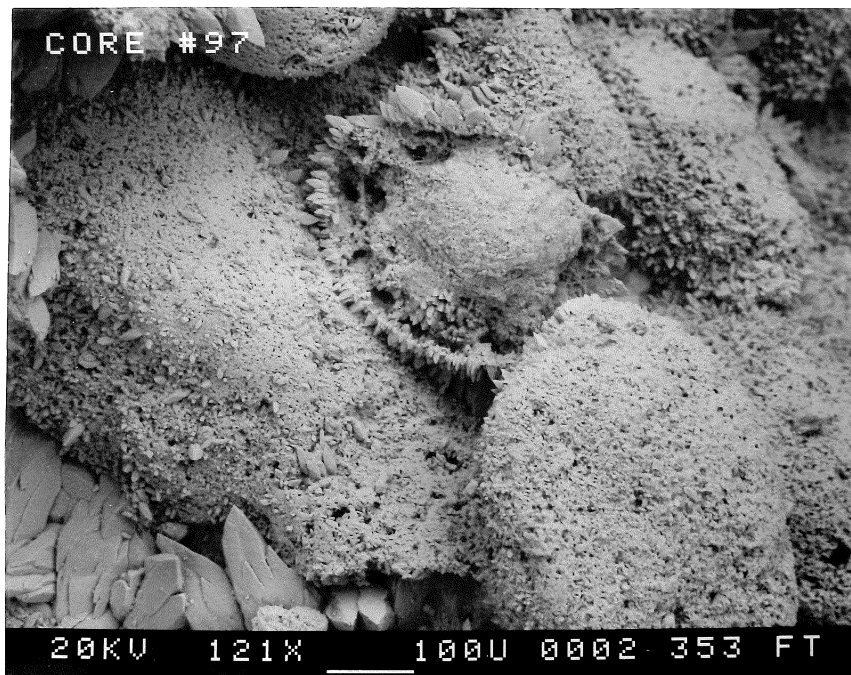
Figure 3. SEM photomicrograph illustrating primary, interparticle
porosity in a foraminiferal, intraclastic packstone with some
intraparticle microporosity within a foraminifera test (center), and
interparticle and intercrystalline microporosity. Foraminiferal test
is coated by outward projecting euhedral, calcite scalenohedra.
Blocky, pore-filling calcite occludes an interparticle pore at lower
left. Core 97, sample depth: 353 ft.

13
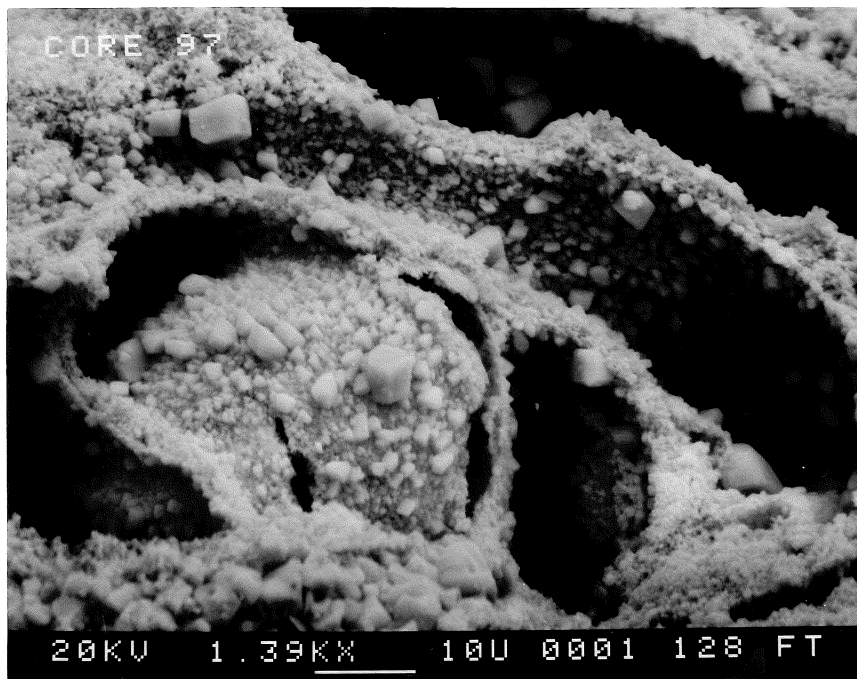
Figure 4. SEM photomicrograph of partially filled chambers of a foraminifera. This intraparticle porosity is in a state of reduction because of the blocky calcite cement filling in these spaces in a fabric-selective way. Core 97, sample depth: 128 ft.
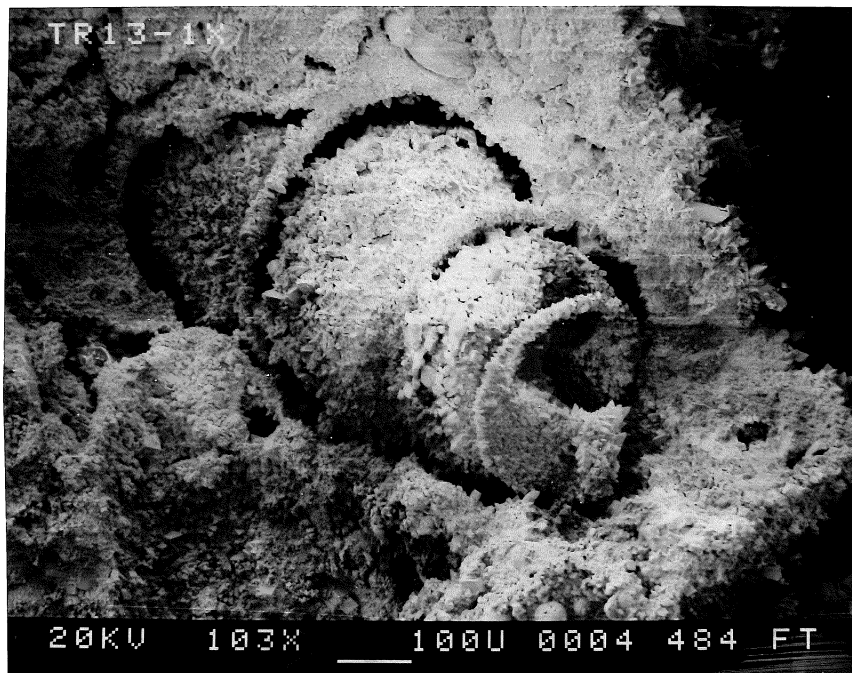
Figure 5. SEM photomicrograph of moldic porosity (fabric-selective). The mold is of a high spired gastropod. Pore walls are presently lined with finely crystalline calcite crystals (less than 10 microns). Core TR13-1X, sample depth: 484 ft.

14
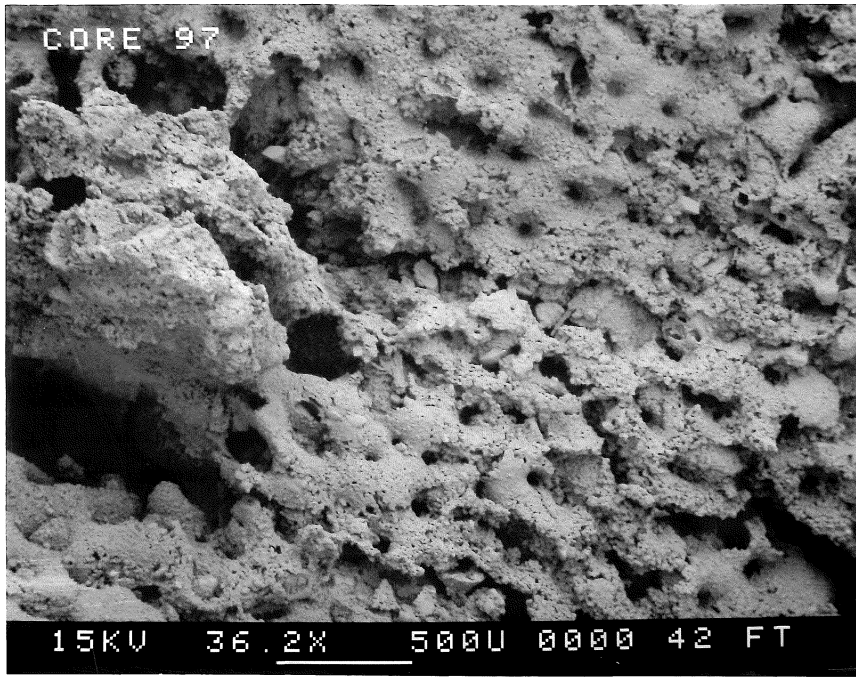
Figure 6.   SEM photomicrograph of fabric-selective growth framework within a reticulated, papillose surface of a coral.   Microcrystalline calcite has coated much of the original growth framework.   This sample is closely associated with moldic and vug porosity.   Core 97, sample depth: 42 ft.
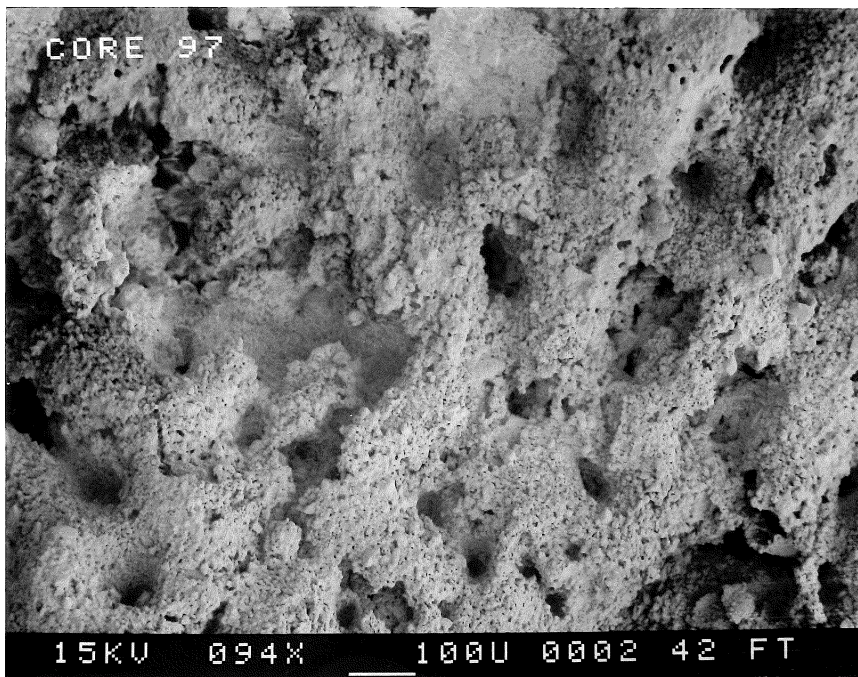
Figure 7.   SEM photomicrograph illustrating a more highly magnified view of Figure 6 showing the partially infilled growth framework porosity.   Core 97, sample depth: 42 ft.
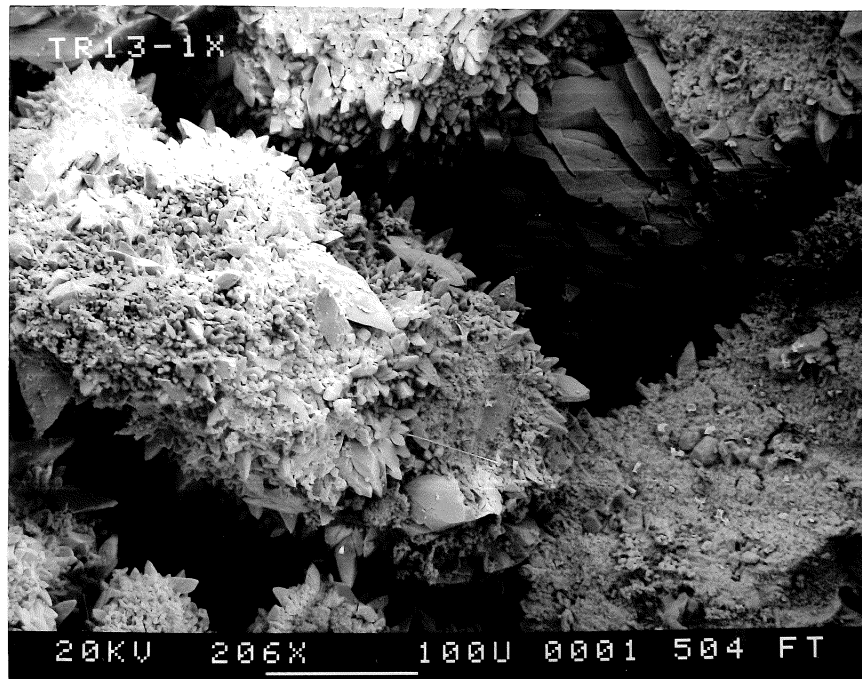
Figure 8.   SEM photomicrograph of "dogtooth", euhedral, calcite
scalenohedra lining an interparticle pore space.   These inward
projecting crystals will eventually coalesce to completely destroy
this pore.   Core TR13-1X, sample depth: 504 ft.
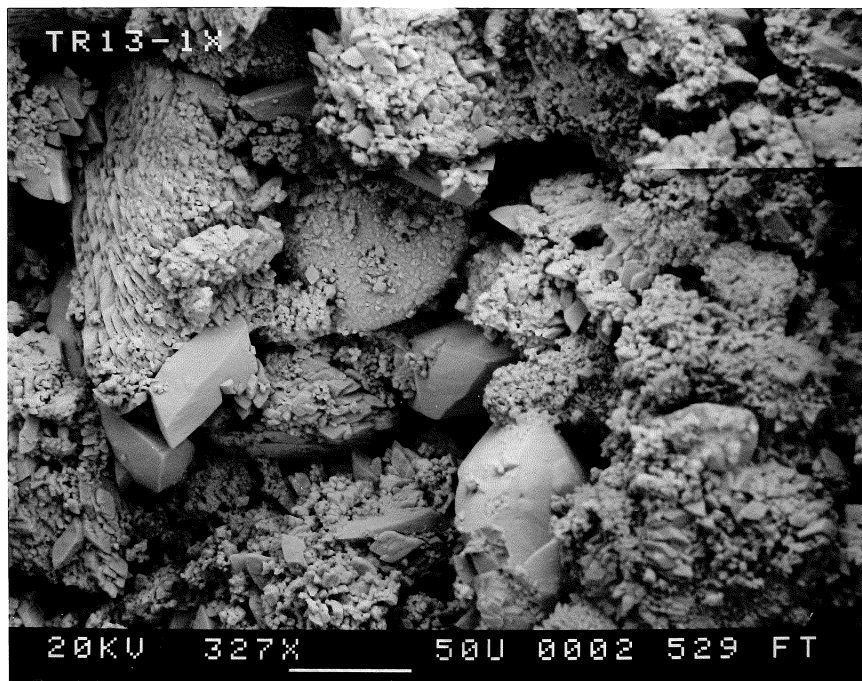
Figure 9.   SEM photomicrograph of interparticle porosity partially
reduced by pore-filling subhedral calcite crystals, approximately 50
microns in size.   These pore-filling crystals have both rhombohedral
and scalenohedral morphologies.   Core TR13-1X, sample depth: 529 ft.

Figure 10. SEM photomicrograph of fracture porosity partially reduced by euhedral scalenohedra of calcite. Core TR13-1X, sample depth: 517 ft.
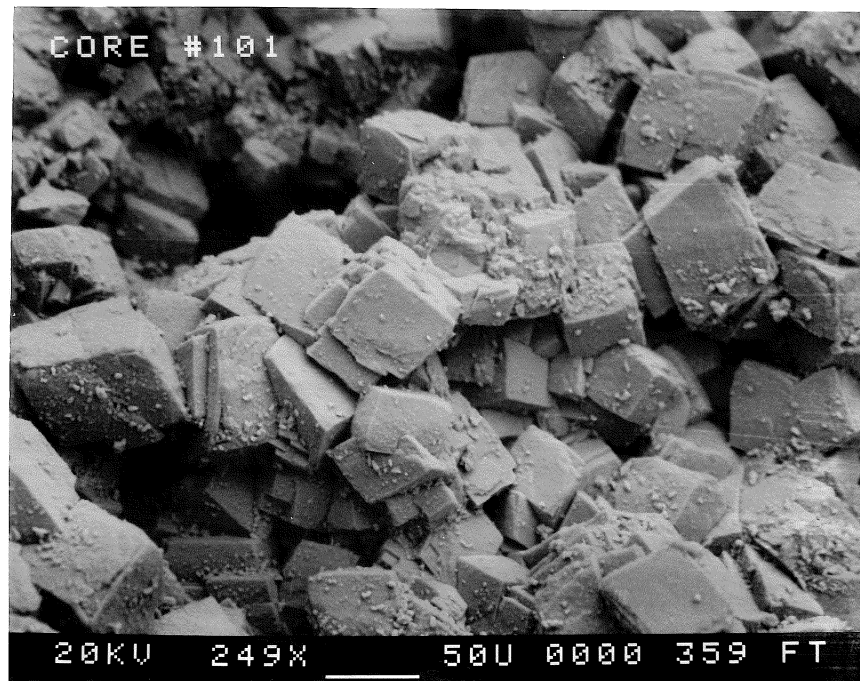
Figure 11. SEM photomicrograph of intergrown euhedral dolomite rhombs lining the surface of a fracture. These rhombs do not exhibit any evidence of deterioration or dissolution. Core 101, sample depth: 359 ft.
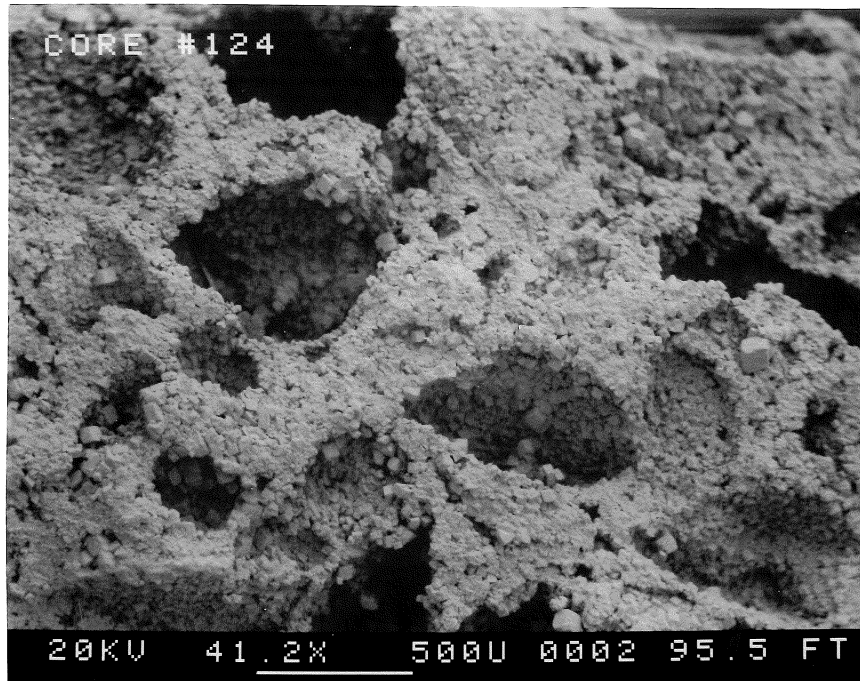
Figure 12. SEM photomicrograph of a foraminifera which has been completely replaced by dolomite. Intraparticle porosity has been partially preserved and intercrystal porosity has been created through dolomitization. Core 124, sample depth: 95.5 ft.
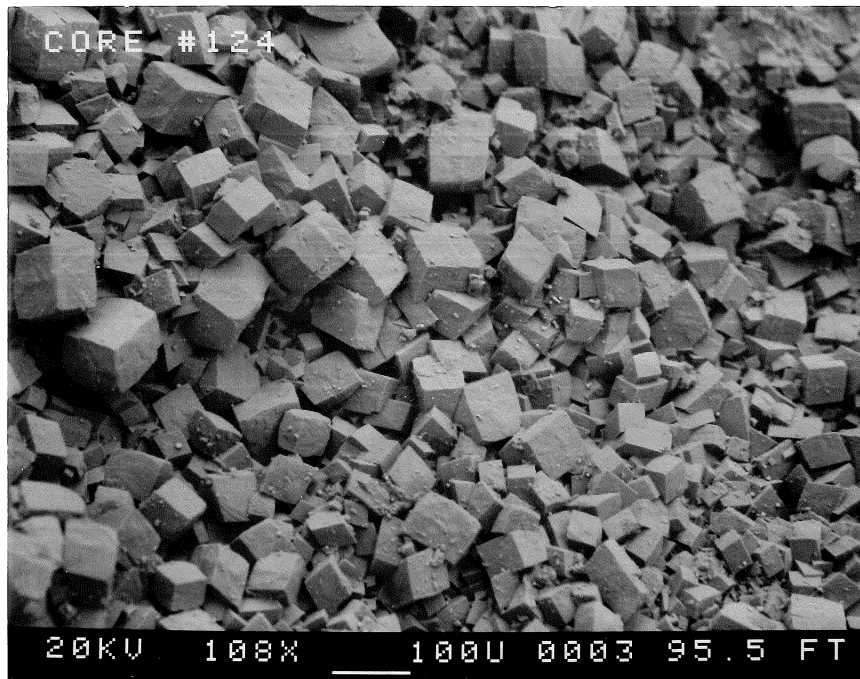
Figure 13. SEM photomicrograph of Figure 12 at a higher magnification showing euhedral rhombs of dolomite intergrown and creating intercrystal porosity. Core 124, sampled depth: 95.5 ft.

Figure 14. SEM photomicrograph of a mosaic of subhedral dolomite crystals lining a vug. These dolomite crystals display varying degrees of corrosion and dissolution and represent the formation of intercrystal porosity and another phase of intracrystal porosity development. Core 124, sample depth: 247.5 ft.
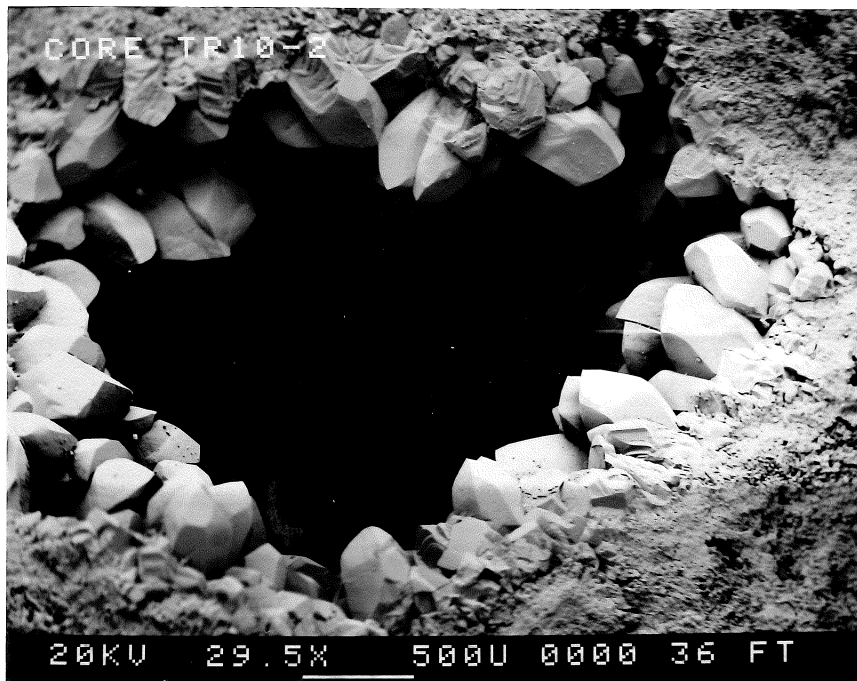
Figure 15. SEM photomicrograph of a large vug which has been partially infilled with medium to coarsely crystalline euhedral calcite crystals. Core TR10-2, sample depth: 36 ft.

19
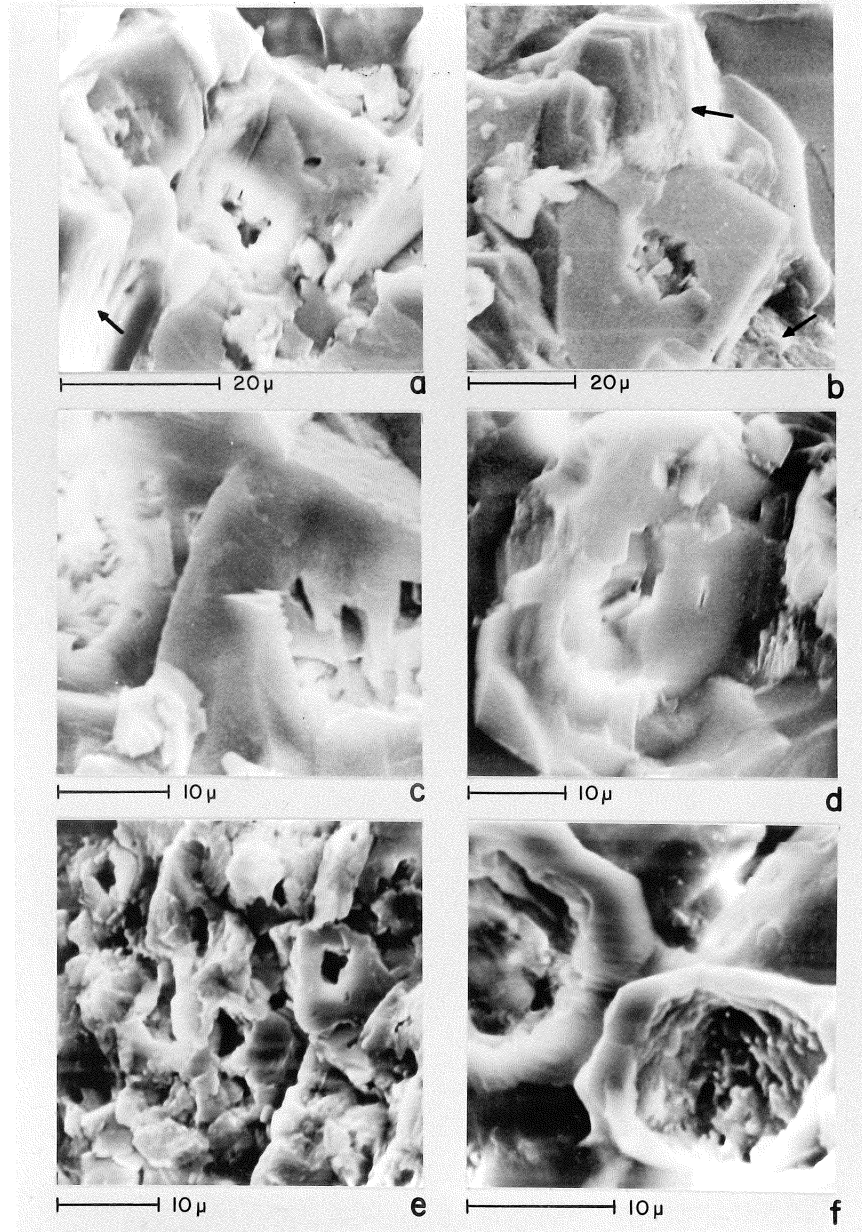
Figure 16. SEM photomicrographs of dolomite crystals displaying extreme dissolution. Most of the dissolution appears to be in the center of these crystals indicating a more calcium-rich area, generally unstable in a fresh water phreatic groundwater system. Arrows in images A and B point to regular cleavage planes or crystal faces developed as a result of phased crystal growth. Core TR18-2, sample depths: A, B, and C - 151.8 meters; D - 172.8 meters; E - 221.6 meters; F - 231.6 meters.
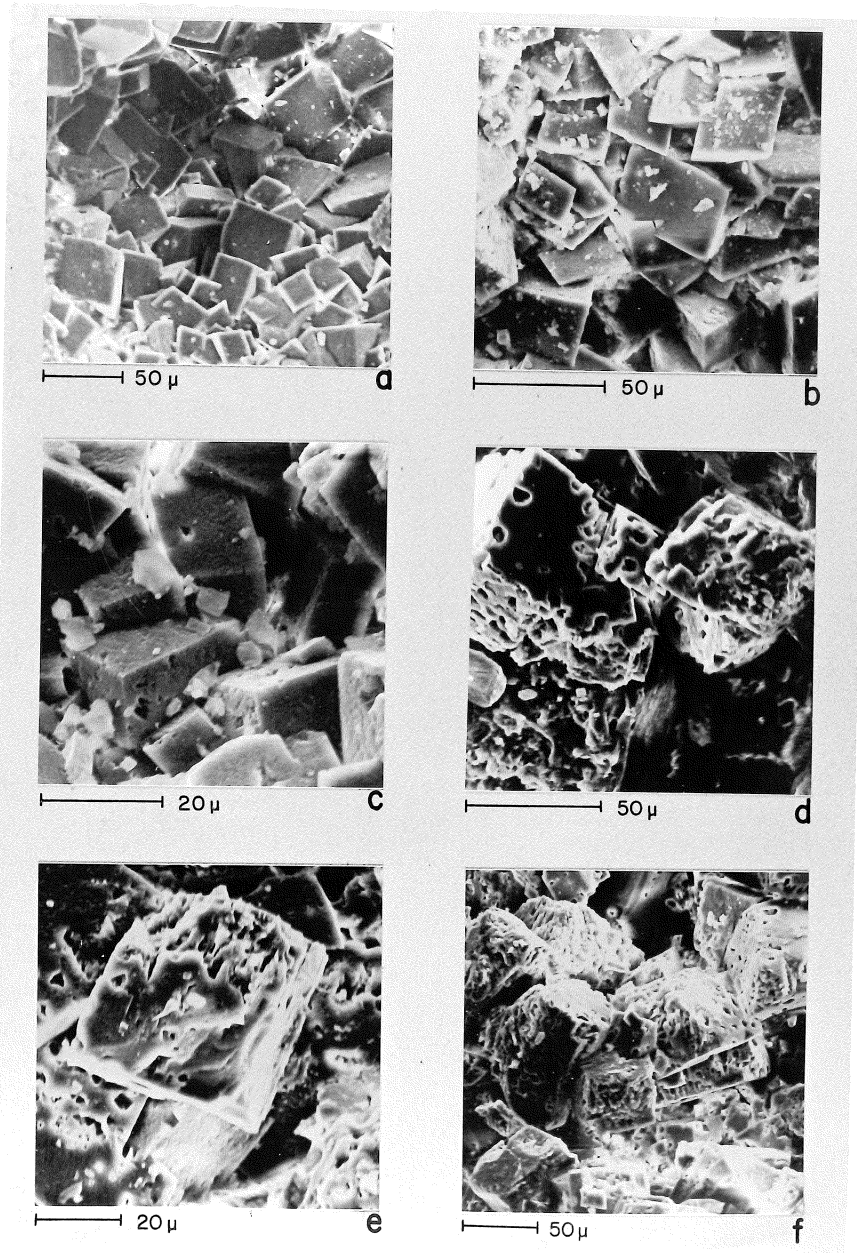
Figure 17. SEM photomicrograph of euhedral pore-filling dolomite from the modern mixing zone. Images A and B display dolomite mosaics of crystals with no apparent corrosion or dissolution. Images C-F display extensive dissolution and corrosion of the crystals. Core TR18-2, sample depths: A and B - 156 meters; C-F - 153.6 meters.

Global sea level changes have affected the Tertiary carbonate rocks of Florida for more than 40 million years. Lower sea level stands resulted in greater surface exposure and extensive changes in the positions and extent of vadose, fresh water phreatic, and marine conditions. Diagenesis of carbonate sediments can begin almost immediately after deposition in a marine environment. Micritization, compaction, and cementation are among the earlier diagenetic processes operating. Subsequent exposure to meteoric conditions (after a sea level drop) will often bring about a period of dissolution of grains composed of unstable minerals (principally aragonite) and further cementation. Replacement of previously dissolved material by dolomite, calcite and silica is common. Thus, pore space evolution is a dynamic, ever changing process. The following discussion of diagenetic processes operating in the coastal carbonate aquifer system of west central Florida focuses on five specific cores (c.f. Randazzo and Cook, 1987; Aardema, 1987; Quinn, 1988).

MICRITIZATION

Micritization is the replacement of original carbonate minerals by microcrystalline calcite (micrite-Folk, 1962) or aragonite. This process generally occurs in the marine environment by algal boring of fossil hard parts and subsequent infilling of the bored areas with micrite (Fig. 2). The process has been well explained by Bathurst

(1975), Kobluk and Risk (1977), and James and Choquette (1984).

Foraminifers are the most commonly micritized grains. They are usually completely micritized. Those that are partially micritized appear to have undergone the process from the center of their tests toward their peripheries. This may be the result of precipitation of calcium carbonate because of bacterial action with decaying organic matter (Wolf, 1965). Often a micrite envelope develops over the grains, particularly coralline algae, foraminfers, and mollusks. These envelopes serve a constructive purpose, as they may survive later dissolution of the grain and preserve the original external shape (moldic porosity) (Fig. 4).

COMPACTION

Evidence of post-depositional compaction of sediment is very limited. Grains usually do not display fracturing or physical displacement. Organic-rich lamination may indicate some compaction of original organic material. The lack of deep burial and early phases of lithification (micritization, marine cementation), as well as inversion of aragonite to calcite (producing a "cushioning effect" of a 8.5% volume increase) account for the minor effects of compaction on porosity. Physical closing of original pore spaces by compaction was not able to be documented visually.

DISSOLUTION

Dissolution is an ever-occurring process because carbonate mineralogics have different solubilities. Thus, it can occur under both marine and non-marine conditions. The coastal area has been repeatedly subjected to marine (saline), transitional (mixing), and nonmarine (fresh) solutions, in response to sea level changes. These solutions are variably saturated and undersaturated with respect to different carbonate minerals. Dissolution of carbonate grains is most apparent in dolomitized sections of the aquifer, reflecting the dissolution phase for dolomite replacement to occur. Saturation with respect to dolomite and undersaturated with respect to calcite have been reported for the coastal mixing zone (Hanshaw and Back, 1979; Land, 1975). Calcite dissolution in the mixing zone has been noted in the Yucatan Peninsula, Mexico (Back and Hanshaw, 1970; Back et. al., 1986; Stoessell et al., 1989).

Noncavernous porosity of the aquifer rocks is the result of these varying conditions. The absence of aragonite in the aquifer rocks indicates significant dissolution since deposition (Figs. 3 and 5). Likewise, the partial to complete dissolution of calcite grains occurs in dolomitized sections of the aquifer. This dissolution may have occurred in the mixing zone.

CEMENTATION

Cementation of carbonate grains by sparry calcite is generally represented by several cement morphologies. Isopachous, scalenohedral crystals oriented with their long axes perpendicular to grains are common as interparticle pore space fillings. The origin of this cement type as marine or nonmarine is equivocal (James and Choquette, 1984).

A second cement type present is pendulous. This form displays greater thicknesses in a downward direction and is believed to form in a meteoric vadose zone under gravitational influences (Longman, 1980).

Blocky, pore-filling calcite cement is locally common (Figs. 3 and 4). Interparticle pore spaces are occluded by these equant crystals. The origin of this cement type is also equivocal, having been reported for the meteoric phreatic (Longman, 1980) and vadose (James and Choquette, 1984) environments.

Micritic cements are presented as isopachous rims around grains and closely associated with micrite envelopes and micritized grains. The fine-grained nature of these cements is quite striking as dark patches or rims. Like others, this cement type may be of a marine or nonmarine origin. Fibrous calcite cements are often associated with micritic cements and are common in marine environments where magnesium ions are abundant.

Often combinations of these types occur within the same rock (Quinn, 1988). Scalenohedral crystals have been seen overlying micritic, isopachous cement and may reflect freshwater cementation following marine. Well-developed syntaxial cements may be found in the same microfacies as equant or blocky and scalenohedral pore-filling crystals. This association, in conjunction with poreward coursening of crystals, suggests freshwater phreatic conditions. The lower Ocala Limestone generally contains more cement combinations characteristic of freshwater phreatic formations. The upper Ocala Limestone, as well as the Suwannee and Avon Park formations, have more variably developed isolated scalenohedra and syntaxial overgrowth indicating more limited development of meteoric cementation. Dolomite and silica cements also occur but will be discussed in the section on replacement.

REPLACEMENT

Replacement of one mineral species by another usually results in a major change of porosity. Dolomite (dolomitization), calcite (calcitization), and quartz (silicification) are the principal minerals involved in the process.

Among these, dolomitization has had the most significant effect on porosity development. Dolomite occurs almost exclusively in the Avon Park, lower Ocala and parts of the Suwannee formations.

Avon Park and Lower Ocala Dolomite. Dolomite crystal sizes range from 0.002 mm to 0.25 mm. Crystals are mostly subhedral and inequigranular. They are generally larger around the periphery of pore spaces. Dolomite fabrics are variable, with features of several fabric types (Randazzo and Zachos, 1984) occurring within the same thin section. Quinn (1988) reports moldic porosity, characteristic of equigranular sieve mosaic fabrics, associated with inequigranular fogged mosaic fabrics. She concludes that the resulting fabrics may be a reflection of the degree of earlier dissolution. Different sequences of dissolution produce different opportunities for dolomite crystallization.

Suwannee Dolomite - Aardema (1987) and Quinn (1988) are among the first to describe petrographically dolomite from the Suwannee Limestone. The dolomite is generally finer grained but equigranular fabrics are more common. Dolomite occurs in mudstone microfacies. Dolomite crystals intersect calcite cement indicating formation during a later stage of diagenesis. Pore spaces are only occasionally rimmed by dolomite crystals suggesting more than one phase of dolomitization.

SEM and Microprobe Characteristics. SEM images reflect the pore-filling characteristics of dolomite. A great deal of variance can be recognized. Core TR 18-2 (Hernando County) contains dolomite crystals with varying degrees of

27

dissolution features, including marked corrosion of crystal centers. Intracrystal dissolution ranged from minor micropore penetration of crystal surfaces, to extensive dissolution of unstable (Ca-rich) crystal centers (Randazzo and Cook, 1987). Cores TR 3-3 (Charlotte County), TR 13-2X (Pinellas County), ROMP 17 (Desoto County) and TR 13-1X (Pinellas County) did not reveal dolomite crystals having these dissolution features (Aardema, 1987; Quinn, 1988). In fact, only calcite crystals from these other cores showed marred or dissolution surfaces.

Microprobe analyses of dolomite crystals (Tables 2-4) from these five cores produced results in keeping with the observed differences in their dissolution. Dolomite from core TR 18-2 had more calcium-rich centers while no recognizable trends or differences could be found for the other four cores.

Trace Element Geochemistry and Stable Isotope Analyses –
Atomic absorption spectrometry was used to determine concentrations of Na and Sr in cores TR 13-2X, TR 3-3, and ROMP 17. Results (Table 5) were somewhat higher than those obtained in earlier studies (Randazzo and Hickey, 1978; Randazzo et al., 1983; Randazzo and Bloom, 1985). These concentrations of Na and Sr suggest a commonality of diagenetic processes affecting the younger (Oligocene) aquifer carbonate rocks. However, the values were appreciably lower than modern marine values and may reflect the phreatic (nonmarine) conditions of diagenesis.

28

Table 2. Dolomite Crystal Microprobe Traverses.* Core TR-18-2 (Randazzo and Cook, 1987)

Traverse	Sample Depth (m)	Mole Percent $CaCO_3$							
		Rim		Center			Rim		
1	152	52.9	52.8	53.2	54.2	53.1	51.8		51.4
2	152	51.4		51.6	52.5		51.1		
3	152	52.7		53.5	52.6		51.1		
7	156	51.8		53.8	55.0	56.8			
8	156	51.8	52.8	54.7					
9	175			52.8	43.0		50.9		
10	175	51.4		52.2	52.8		51.4		

*Values in mole percent $CaCO_3$ from ZAF data reduction of 10 micron spot analyses.

Standard deviation of K (X-ray intensity ratio relative to standard specimen) ranged from 0.50 to 0.59 percent.

29

Table 3. Dolomite Crystal Electron Microscope Analysis (Aardema, 1987)

Core/Sample No.	Depth Below Ground Surface (M)	Mean Mole % MgCo
TR13 2X-8-A	152.1	46
TR13 2X-8-B		45
TR13 2X-9-A		45
TR13 2X-9-B	153.8	45
TR13 2X-9-C		45
Romp 17-8-A		47
Romp 17-8-B	248.9	42
Romp 17-8-C		46
Romp 17-10-A		44
Romp 17-10-B	249.8	46
Romp 17-10-C		45
TR3-5-A		45
TR3-5-B	278.5	46
TR3-5-C		49
TR3-10-A		47
TR3-10-B	281.2	45
TR3-10-C		46

Table 4. Dolomite crystal microprobe traverses (Quinn, 1988).

Sample:	7	7	7	8	8	8	35-35A
Crystal:	1	2	3	1	2	3	1
Traverse length:	33.01 µ	44.64 µ	31.90 µ	32.00 µ	44.00 µ	15.00 µ	
point:	mol% $MgCO_3$	mol% $MgCO_3$	mol% $MgCO_3$	mol% $MgCO_3$	mol% $MgCO_3$	mol% $MgCO_3$	mol% $MgCO_3$
1	44.2	46.4	43.7	46.1	47.0	46.7	50.0
2	44.1	46.6	43.7	46.1	47.1	46.7	44.5
3	43.9	45.5	43.7	46.8	47.7	47.1	44.8
4	44.6	46.2	45.2	45.6	47.3	46.3	44.7
5	45.1	46.2	43.6	45.2	47.4	47.7	44.5
6	44.4	45.0	44.4	46.2	48.0		44.2
7	44.4	44.9	45.7	45.8	47.7		44.6
8	45.2	45.6	45.5	45.6	47.3		43.9
9	44.1	46.5	45.2	45.9	47.3		44.7
10		46.8	42.7	45.6	47.2		44.3
11			43.8		48.1		45.3
11			43.8		48.1		45.3
12			43.2		47.5		46.9
13			43.9		47.6		45.7
14			43.6		48.1		46.0
15			44.7		48.2		47.2
16					47.9		45.8
17					47.4		45.8
18					47.8		44.5
19					46.9		44.3
20					47.3		50.5

Note: All samples were analyzed for mol% $CaCO_3$; values for mol% $CaCO_3$ equal difference between mol% $MgCO_3$ and 100%.

31

Table 4. (continued)

Sample: Crystal: Traverse length: point:	35-35A 2 55.00 μ mol% $MgCO_3$	35-35A 3 62.00 μ mol% $MgCO_3$	37 1 80.45 μ mol% $MgCO_3$	37 2 74.06 μ mol% $MgCO_3$	37 3 55.13 μ mol% $MgCO_3$	37 4 40.80 μ mol% $MgCO_3$	43 1 mol% $MgCO_3$
1	45.8	44.7	44.7	43.9	45.1	43.8	46.5
2	45.9	45.9	45.2	44.0	45.0	44.9	45.6
3	45.7	46.2	45.1	43.8	45.2	44.6	45.7
4	46.4	45.7	44.5	44.0	44.9	45.1	45.3
5	46.5	46.1	45.6	43.4	45.0	45.2	45.2
6	46.6	45.3	45.6	44.4	44.8	45.1	45.9
7	46.4	46.1	44.7	44.2	44.5	45.2	45.0
8	46.1	45.8	46.3	44.5	44.7	45.3	46.5
9	45.4	39.3	44.5	43.9	44.0	45.4	46.1
10	45.0	19.0	45.8	44.2	44.5	46.7	39.0
11	45.4	37.8	46.0	44.3	44.4		46.2
12	46.0	45.2	45.3	44.1	44.6		45.4
13	45.7	46.0	45.6	44.1	44.5		46.4
14	45.5	44.8	44.6	44.3	45.0		47.1
15	45.8	46.0	44.7	44.7	45.2		48.3
16	45.2	46.0	45.4	44.1			
17	45.1	45.0	45.9	43.9			
18	45.3	41.3	45.7	43.9			
19	45.5	45.9	45.9	44.5			
20	45.5	45.8	45.9	44.6			

Table 4. (continued)

point:	Sample: 43 Crystal: 2 Traverse length: 72.00 μ mol% $MgCO_3$	43 3 67.00 μ mol% $MgCO_3$	47 1 59.40 μ mol% $MgCO_3$	47 2 101.40 μ mol% $MgCO_3$	48 1 80.00 μ mol% $MgCO_3$	48 2 30.00 μ mol% $MgCO_3$	48 3 85.00 μ mol% $MgCO_3$
1	48.0	46.0	47.6	49.2	43.8	44.8	46.3
2	47.6	46.1	44.9	45.4	44.5	44.9	44.6
3	46.0	45.5	44.0	44.6	44.9	45.4	44.8
4	46.2	44.9	43.9	45.4	44.1	44.8	44.9
5	46.2	45.9	43.8	45.2	43.4	32.6	44.7
6	45.6	45.2	43.8	44.4	43.2	44.4	45.6
7	45.5	43.2	43.7	45.1	43.6		44.5
8	45.7	45.1	44.3	43.0	43.7		44.5
9	45.3	45.3	43.6	44.9	43.3		44.4
10	45.0	45.0	43.8	41.8			44.8
11	45.9	45.4					
12	45.1	45.7					
13	45.3	45.7					
14	44.4	45.1					
15	46.0	45.5					
16	46.7	45.0					
17	46.7	46.2					
18	48.4	44.7					
19	47.6	45.7					
20	49.4	45.1					

33

Table 4. (continued)

Sample: Crystal: Traverse length: point:	52 1 40.00 μ mol% MgCO$_3$	52 2 47.00 μ mol% MgCO$_3$	52 3 108.00 μ mol% MgCO$_3$	54 1 30.000 μ mol% MgCO$_3$	54 2 56.60 μ mol% MgCO$_3$	54 3 25.00 μ mol% MgCO$_3$
1	49.1	49.6	52.0	47.2	47.2	44.7
2	47.9	48.6	44.4	46.3	47.7	46.0
3	46.9	48.7	44.0	46.5	46.2	44.9
4	46.9	48.6	43.6	46.1	46.1	46.0
5	47.7	49.7	43.7	46.0	46.7	45.7
6	46.7	48.7	47.4	45.6	45.2	46.8
7	46.4	45.8	43.8	45.9	46.2	46.0
8	47.1	46.0	42.8	46.3	47.0	46.4
9	47.7	46.1	42.9	46.2	46.1	46.2
10	46.8	47.0	44.9	46.2	46.2	46.0
11				46.2	46.6	
12					46.0	
13					46.9	
14					47.9	
15					49.0	

34

Table 4. (continued)

Sample:	55	55
Crystal:	1	2
Traverse length:	44.00 μ	52.00 μ
point:	mol% $MgCO_3$	mol% $MgCO_3$
1	47.0	48.3
2	45.9	45.7
3	45.8	45.7
4	45.7	45.9
5	45.5	45.3
6	45.9	45.1
7	45.7	44.1
8	45.8	45.6
9	45.2	45.0
10	45.9	44.5

Table 5. Sodium and Strontium Trace Element Concentrations (Aardema, 1987)

Core/Sample No.	Depth Below Ground Surface (M)	Na (ppm)	Sr (ppm)
TR13-2X-8	152.1	1233	360
2X-9	153.8	1089	330
2X-10	154.9	1156	335
Romp-17-9	249.5	544	360
17-10	249.8	428	330
TR3-5	278.5	1344	410
TR3-9	279.9	939	544
TR3-11	281.3	1417	386

Stable isotope analyses of calcite and dolomite

crystals for cores TR 18-2, TR 13-2X, TR 3-3, and ROMP 17

revealed (Table 6-7) enriched (heavy) and depleted (light)

values. Dolomite values for $\delta^{18}O$ were generally enriched

for all samples while calcite was depleted. Carbon ($\delta^{13}C$)

values for dolomite and calcite varied from depleted to

enriched. These variances in stable isotope compositions

may be attributable to inherited C13 from precursor

sediments and the influence of abundant organic matter.

Reequilibration under meteoric conditions through time may

be responsible for the values reported.

Silicification - Silicification, the replacement of earlier

formed minerals by quartz, occurs on a minor scale. It is

principally limited to occasional replacement or selected

carbonate grains or infilling of a dissolution vug. This

process appears to be a late diagenetic occurrence as

partial replacement of calcite and dolomite grains and

overgrowths. Silica solubility is influenced by

temperatures and pH (Friedman and Sanders, 1978). High pH

values, conducive to its solubility, have been associated

with the aquifer. Sources of silica include clay minerals

and detrital quartz. Silicification represents a

destructive porosity process.

PERMEABILITY

Permeability is the ability of a rock to transmit

fluids and varies with porosity. While not all high

37

Table 6. Oxygen and Carbon Isotopic Concentrations (Aardema, 1987)

Core/Sample No.	Depth (m) Below Ground Surface	Mineralogy	$\delta^{18}O$	$\delta^{13}C$
TR13-2X-7	151.5	calcite	-1.57	1.23
2X-8	152.1	dolomite	3.90	-2.41
2X-9	153.8	dolomite	3.77	-0.63
2X-10	154.7	dolomite	3.13	6.7
2X-11	157.6	calcite	-2.68	-0.14
Romp-17-7	248.6	calcite	-0.90	0.60
17-9	249.5	dolomite	3.79	-1.42
17-10	249.8	dolomite	3.32	-1.73
17-12	250.2	calcite	-1.17	0.24
TR3-6	278.7	calcite	-3.39	0.17
TR3-7	278.9	calcite	-3.57	0.60
TR3-8	279-4	calcite	-3.76	0.25

Table 7. $\delta 13_C$ and $\delta 18_O$ analyses for core TR 18-2

Sample	Depth (m)	$\delta\underline{13}_C$	$\delta\underline{18}_O$
1	151.8	+2.40	+3.69
3	153.6	+2.75	+3.83
5	156.1	+2.15	+3.54
9	162.5	+2.70	+4.17
18	174.8	+3.10	+3.83
29	202.7	+2.80	+3.88
38	221.6	+1.20	+3.64
47	234.4	+1.30	+3.88
53	245.1	+1.65	+3.50
55	248.1	+1.90	+3.69

$\delta 13_C$ and $\delta 18_O$ values are given as 0/00 vs. the PDB standard.

porosity rocks have high permeability, low porosity generally yields low permeability. Instrumental measurements of permeability, conducted at a commercial laboratory, yielded values up to 25,000 md (Table 8 and Figs. 18-20). Fossilferous limestones had the highest permeability values while dolomite samples had some of the lowest and highest. Positive correlations between relatively high permeability and relatively high visible porosity could be made for the dolomitized sections of core TR18-2 and TR13-1X. Positive correlations between relatively low permeability and relatively low visible porosity could be made for the dolomitized sections of cores TR13-2X and TR3-3. No correlations for these two parameters were apparent for core ROMP17. This probably reflects the varying degrees of diagenetic alteration in dolomite horizons.

Permeability of Holocene sediments from Florida and the Bahamas are as high as 57,000 md (Enos and Sawatsky, 1981). Dolomitization produces the highest permeabilities at 80-90% completion of the replacement process and generally decreases beyond 90% replacement (Murray, 1960; Powers, 1962). Intergranular pores are progressively reduced in size and number during late dolomitization (Wardlaw, 1976). A variance in pore-to-throat size accompanying this reduction produces the lower permeability.

Table 8. Permeability Analysis

Core/ Sample No.	Depth (m) below Ground Surface	Permeability (md)	Lithology
TR13-2X			
-1	129.5	7.00	Limestone
-4	134.1	2657.00	Limestone
-7	151.5	1368.00	Limestone
-8	152.1	0.03	Dolomite
-10	154.9	0.06	Dolomite
-12	160.0	205.00	Limestone
-15	171.5	105.00	Limestone
-25	190.5	76.00	Limestone
-28	199.0	25000.00	Limestone
TR3-3			
-1	274.6	211.00	Limestone
-4	276.7	1045.00	Limestone
-7	278.9	93.00	Limestone
-9	279.9	0.01	Dolomite
-10	281.2	0.01	Dolomite
-12	281.6	0.01	Dolomite
ROMP 17			
-1	243.5	120.00	Limestone
-4	246.4	30.00	Limestone
-7	248.6	9.50	Limestone
-10	249.8	0.03	Dolomite
-13	252.0	367.00	Limestone
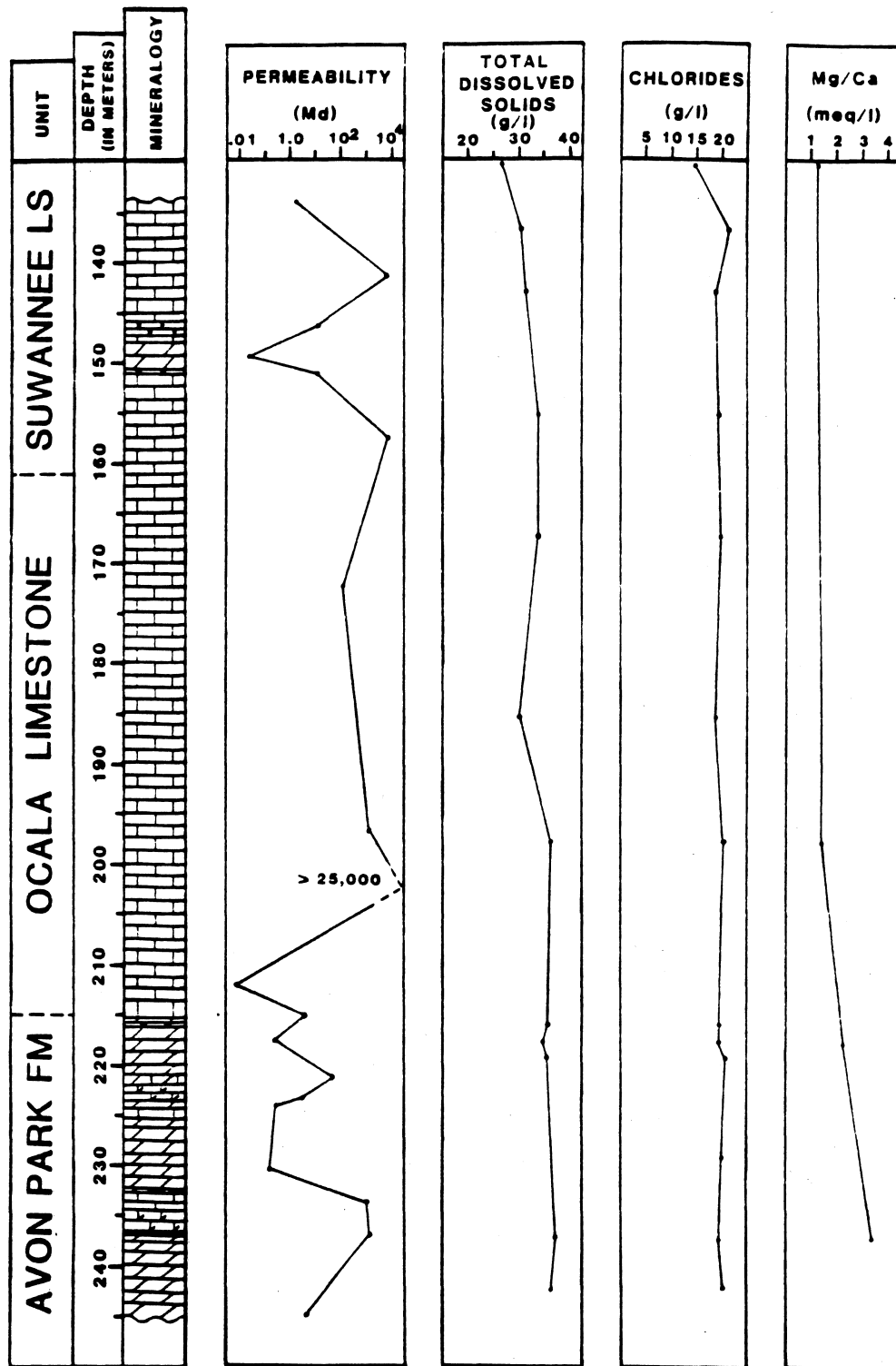
LEGEND

▨ calcite
▨ dolomitic calcite
▨ calcitic dolomite
▨ dolomite

Figure 18. Permeability and limited water quality data from core TR 13-1X. This interval of core is in the saline – slightly hypersaline groundwater zone (after Quinn, 1988).

42
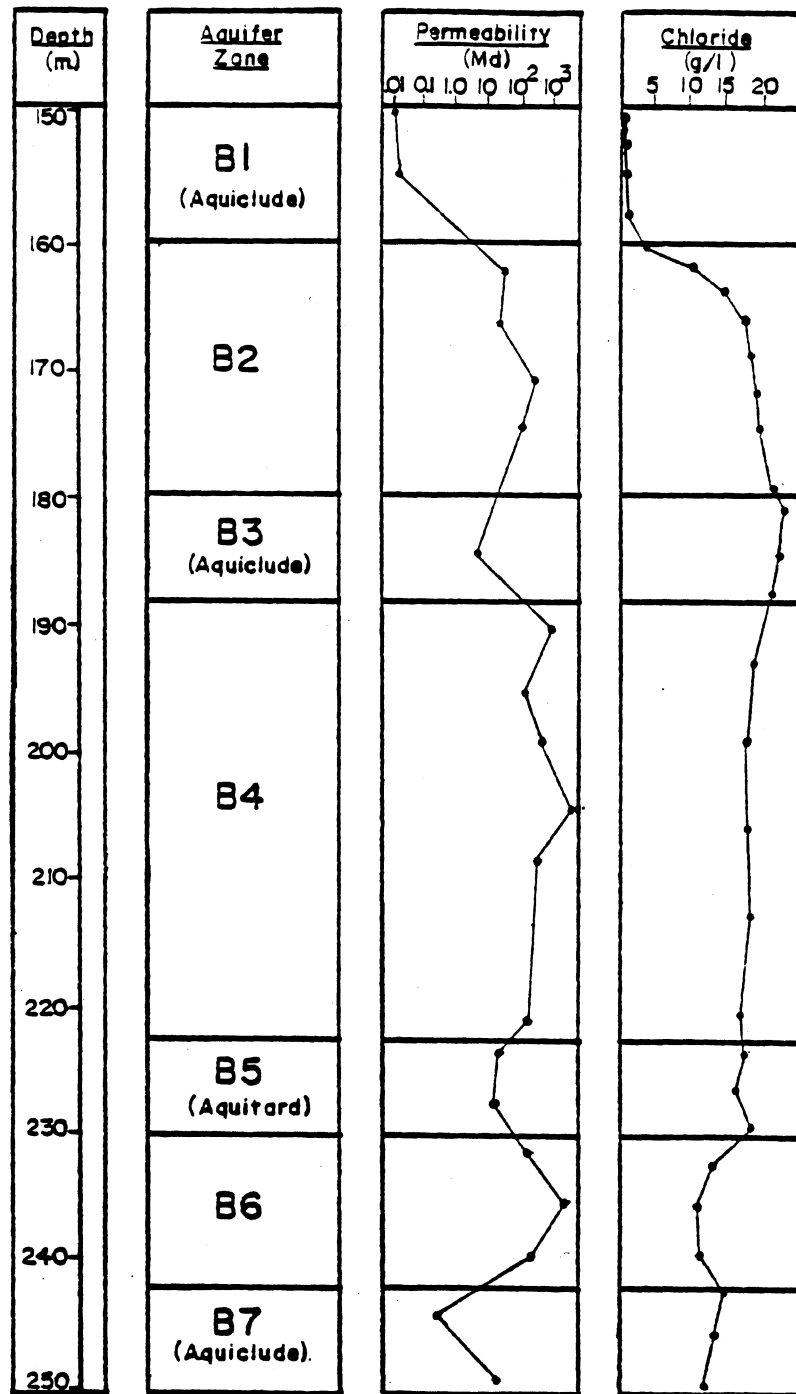
Figure 19. Hydrologic regime of mixing and saline zones of Well TR 18-2. Freshwater phreatic Aquifer Zone A, above this section, averages less than 10 mg/1 chloride.

43
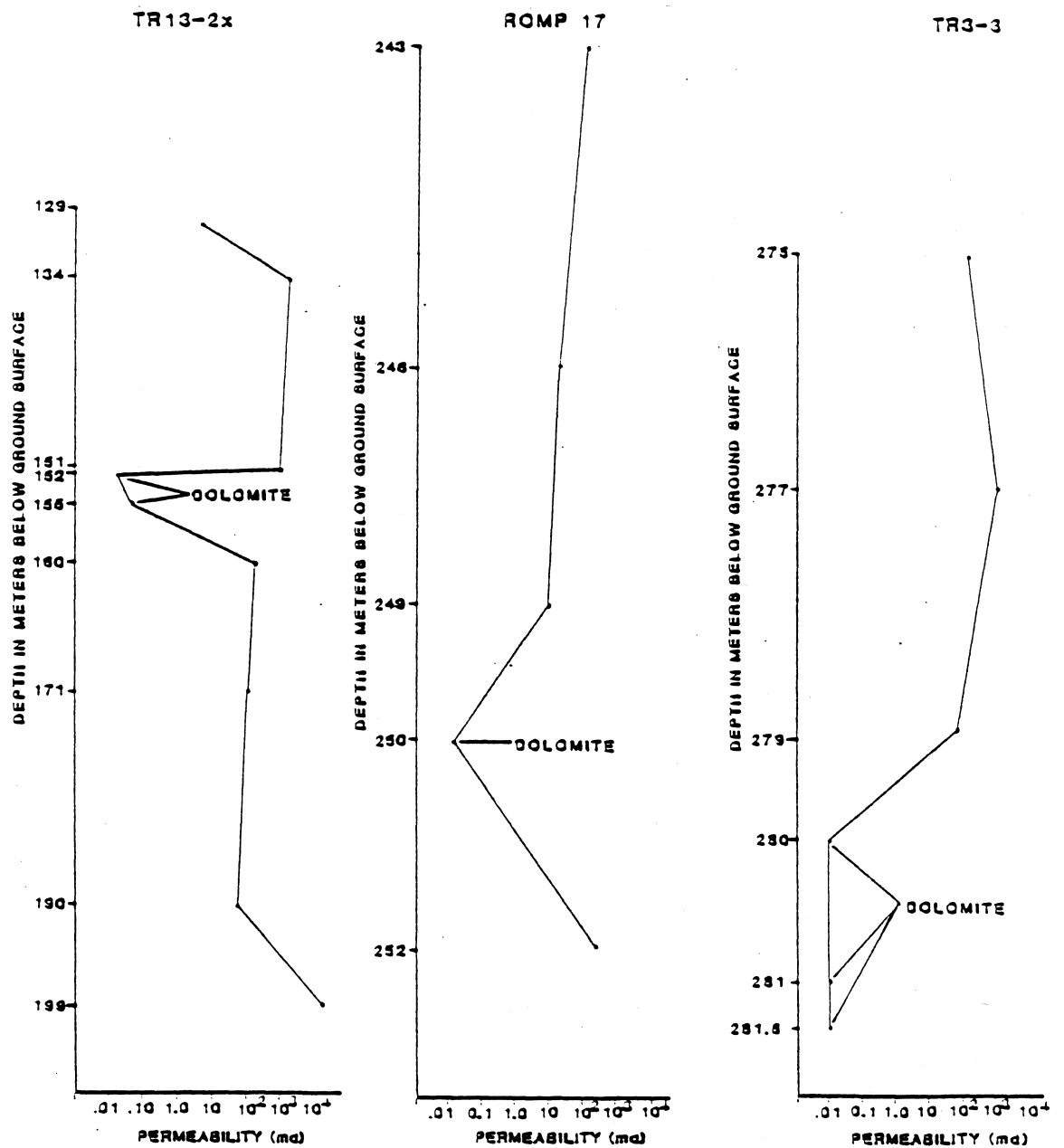
Figure 20. Variations in permeability for cores TR 13-2X, ROMP 17, and TR 3-3. These diagrams illustrate the greatly reduced permeability across the dolomite intervals (after Aardema, 1987).

HYDROGEOLOGY

The Floridan aquifer has several thick, low permeability confining units (Thayer and Miller, 1984) which create anisotropic water flow conditions. Along the west coast of central Florida the upper portion of the aquifer contains portable water occurring as a lens above a brackish water zone (mixing) and a deeper zone of saline to hypersaline water.

Total dissolved solids (TDS), chloride, and sulfate concentrations define these groundwater regimes. Figures 18 and 19 reflect the vertical distribution of some of these parameters. The five cores focused on for this study have different positions in the hydrologic regimes of the aquifer (c.f. Randazzo and Cook, 1987; Aardema, 1987; Quinn, 1988).

Groundwater geochemistry directly controls diagenetic changes in the aquifer rocks. Dissolution and dolomitization, two of the most important processes affecting porosity, are complexly related to the different hydrologic regimes.

A three-phase equilibrium exists among calcite, dolomite, and aqueous solution when the Mg/Ca ratio is approximately one (Hanshaw et al., 1971). The aqueous solution is theoretically supersaturated for dolomite at ratios >1 and dolomitization is favored. Other factors, such as kinetics of the reaction and the presence of competing ions (ionic compositions of the aqueous solution)

also influence the carbonate mineral phase to form (Folk and
Land, 1975; Hanshaw and Back, 1979).

Limited determinations of Mg/Ca ratios reveal values >1
in groundwater of the study area. Plots of Mg/Ca ratios
versus salinity show the fields of occurrence for these
waters (Fig. 21). Data points indicate the calcite should
be precipitating into pore spaces and dolomite should be
dissolving. Visible evidence of dolomite dissolution was
observed in core TR 18-1X but not in core TR 13-1X.

THE MODEL OF POROSITY DEVELOPMENT
A SUMMARY OF DATA AND INTERPRETATIONS

Carbonate sediments were deposited in supratidal,
intertidal, and subtidal environments (equivalent to a
middle shelf carbonate bank) during the Eocene and Oligocene
Epochs. Sea level changes and uplift and downwarping of the
Florida Platform, resulted in responsive shifts of
environmental positions and resulting carbonate depositional
facies. Water energy levels controlled the accumulation of
lime mud. Organic influences, primarily through fossil
remains and bioturbation, interacted with physical
conditions to create primary porosity in the sediments.
Diagenetic (post depositional) processes began immediately
and have continued to the present. The diagenetic processes
responsible for changes in porosity are compaction,
recrystallization (including micritization), inversion,
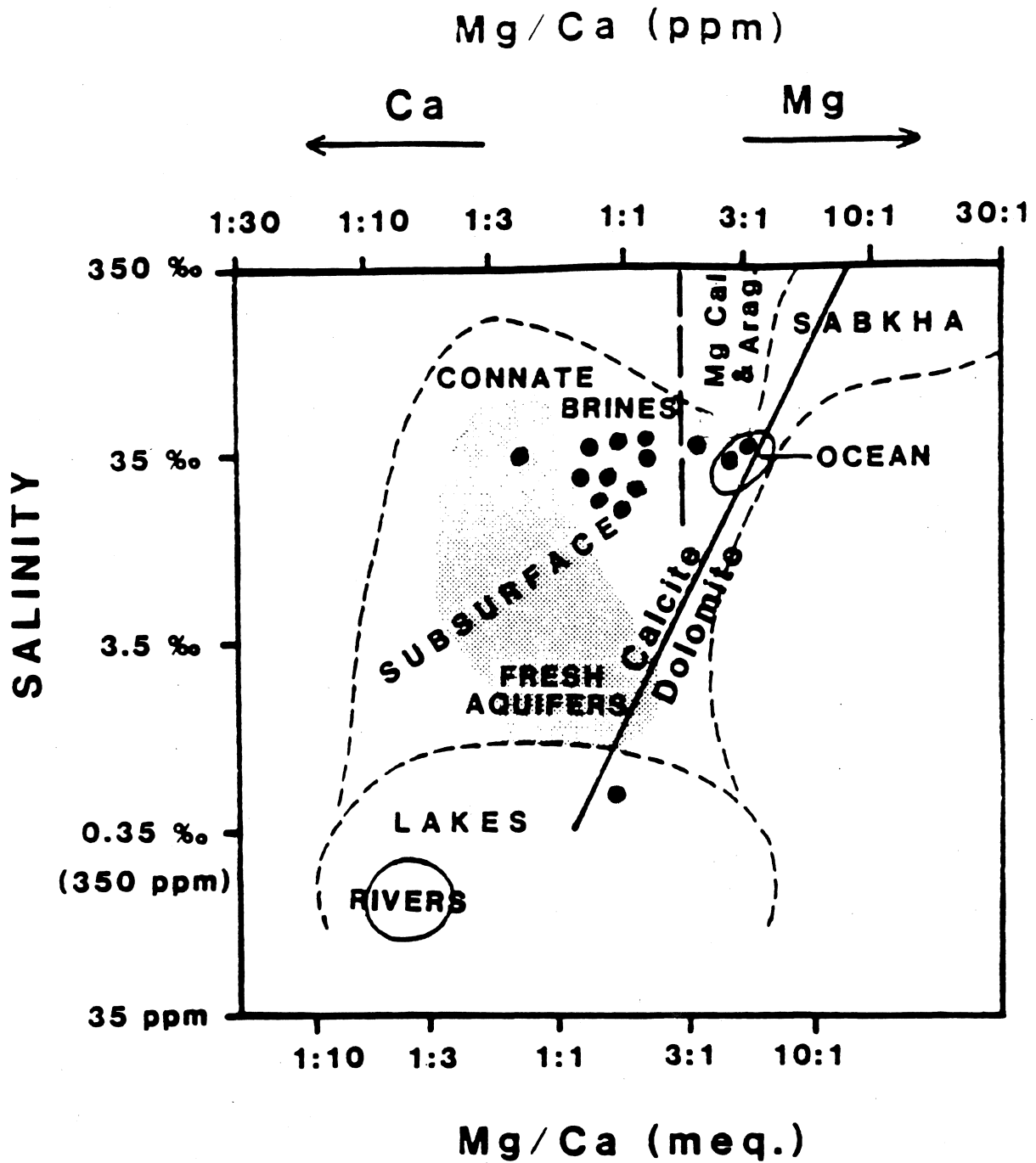
Figure 21. Salinity versus Mg/Ca values for well-water from TR 13-1X and TR 18-2. Fields of occurrences of common natural waters are provided for reference (after Folk and Land, 1975). These data predict calcite to be the preferred carbonate phase. Several data points for well TR 18-2 indicate a preference for magnesium calcite/aragonite. Dolomite is preferred for only one data point in well TR 18-2.

47

cementation, dissolution, and replacement (dolomitization most importantly).

Evolution of porosity in coastal carbonate rocks of the Upper Floridan Aquifer System has been occurring for more than 40 million years. Changing chemical conditions of the groundwater system have responded through time to sea level changes and the seaward and landward migration of the saltwater/freshwater interface (mixing zones). The carbonate aquifer rocks have been subjected to numerous periods of marine and nonmarine phreatic environments, as well as vadose conditions. Carbonate minerals comprising the aquifer rocks reacted to new chemical conditions through the diagenetic processes mentioned and described previously.

The conceptual model developed in this study addresses and evaluates the relationship of porosity to flow paths of groundwater, regional stratigraphy, lithologic and mineralogical distributions, and the geochemistry of groundwater and aquifer rocks. The model attempts to predict how and where porosity is developing today and the chemical and physical conditions responsible for it. Figure 22 depicts the noncavernous porosity distribution of the cores used as the basis of the model.

Porosity and Groundwater Flow - Groundwater flow paths are adequately illustrated in Randazzo and Bloom (1985) for the region studied (Fig. 23). The flow directions reflect the potentiometric maps of the area and depict two major points of groundwater recharge, with discharge seaward as well as

NORTH   SOUTH

TR13-1X   TR13-2X

TR18-2

DEPTH BELOW LAND SURFACE (Meters)

ROMP 17

TR3-3
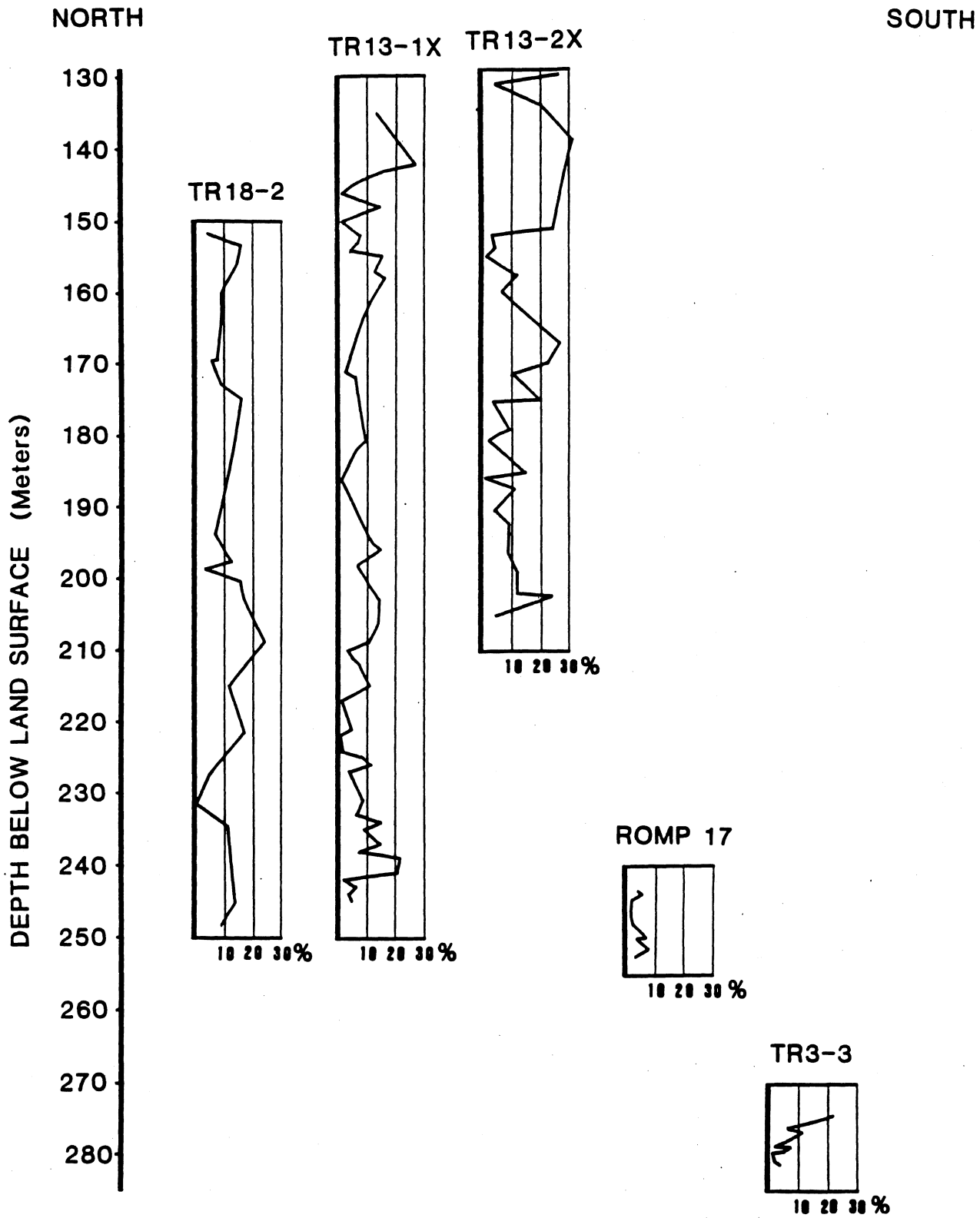
No Horizontal Scale

Figure 22.   TOTAL VISIBLE POROSITY (%)

49
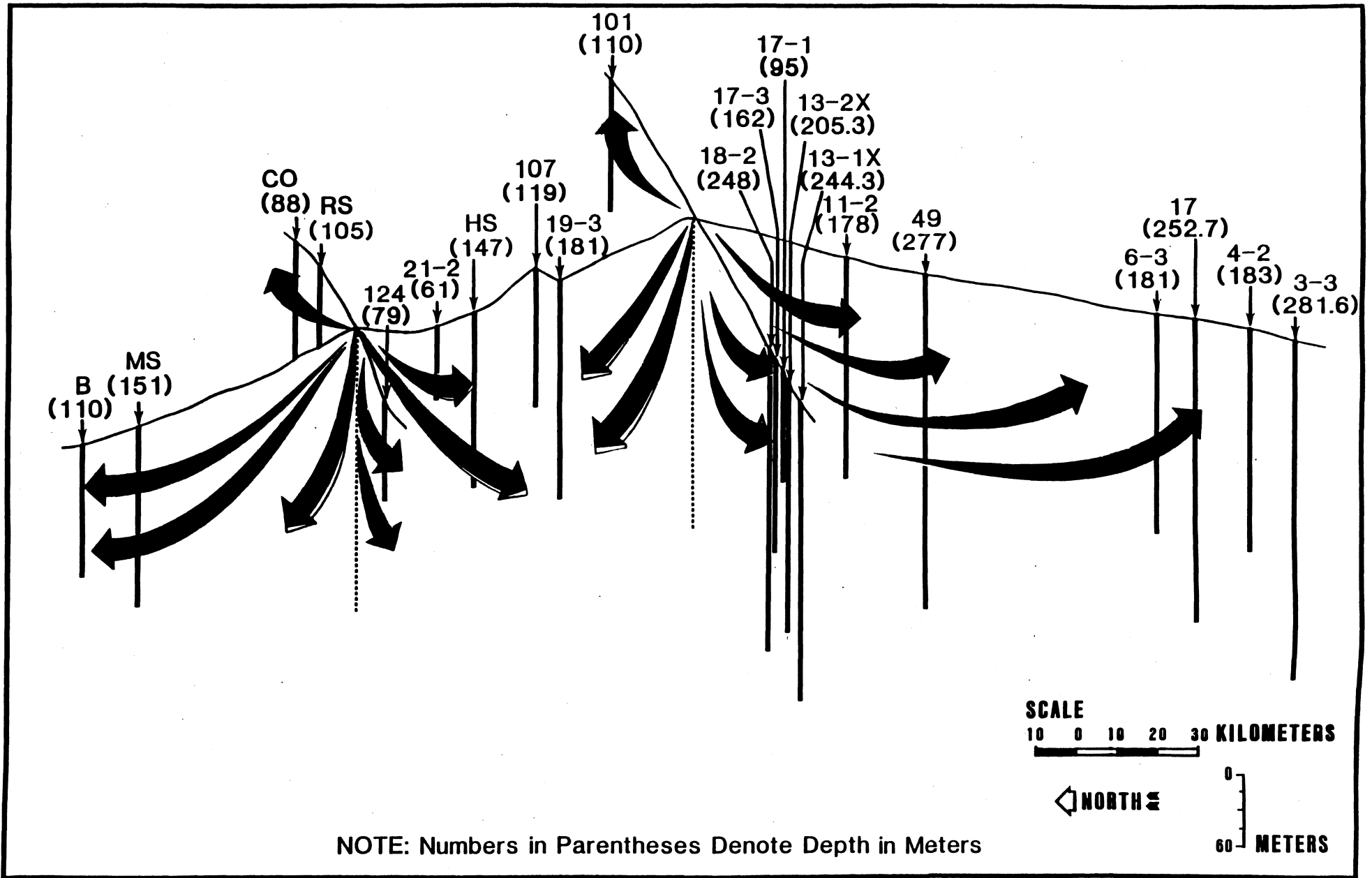
Figure 23. Projected flow of groundwater in the Upper Floridan Aquifer System. Points of origin for the flow lines represent the Levy County (left) and Pasco County (center) recharge areas. Locations for this panel diagram are keyed to Figure 1.

landward. When compared with Figure 22, it shows, through extrapolated data, the direct relationship between these aspects of the coastal aquifer. Cavernous porosity (not included in the model) is a significant factor which can account for discrepancies in the direct porosity/groundwater flow relationship.

As described earlier, groundwater flow direction, as well as volume, are controlled to an even greater extent by permeability. Visible noncavernous porosity, observed through light microscope and SEM, reveal aspects of permeability by the interconnectiveness, size, and frequency of pores. Such observations provide an understanding of the subtle, yet important role played by porosity types, abundances, and distribution. Comparisons of Figure 22 with permeability data plotted in Figures 18-20 show both positive and negative correlations. These are the result of the complex diagenetic processes constantly in operation in the water/rock interactions of the Floridan Aquifer System.

Porosity and Stratigraphy - Regional stratigraphy for the Upper Florida Aquifer System is represented by the Avon Park Formation and the Ocala and Suwannee Limestones (Fig. 24). These carbonate units are composed of numerous lithofacies. The strata dip and thicken to the south and west (coast), away from the Peninsular Arch, a southerly trending structural high paralleling the axis of peninsular Florida (Vernon, 1951; Chen, 1965).
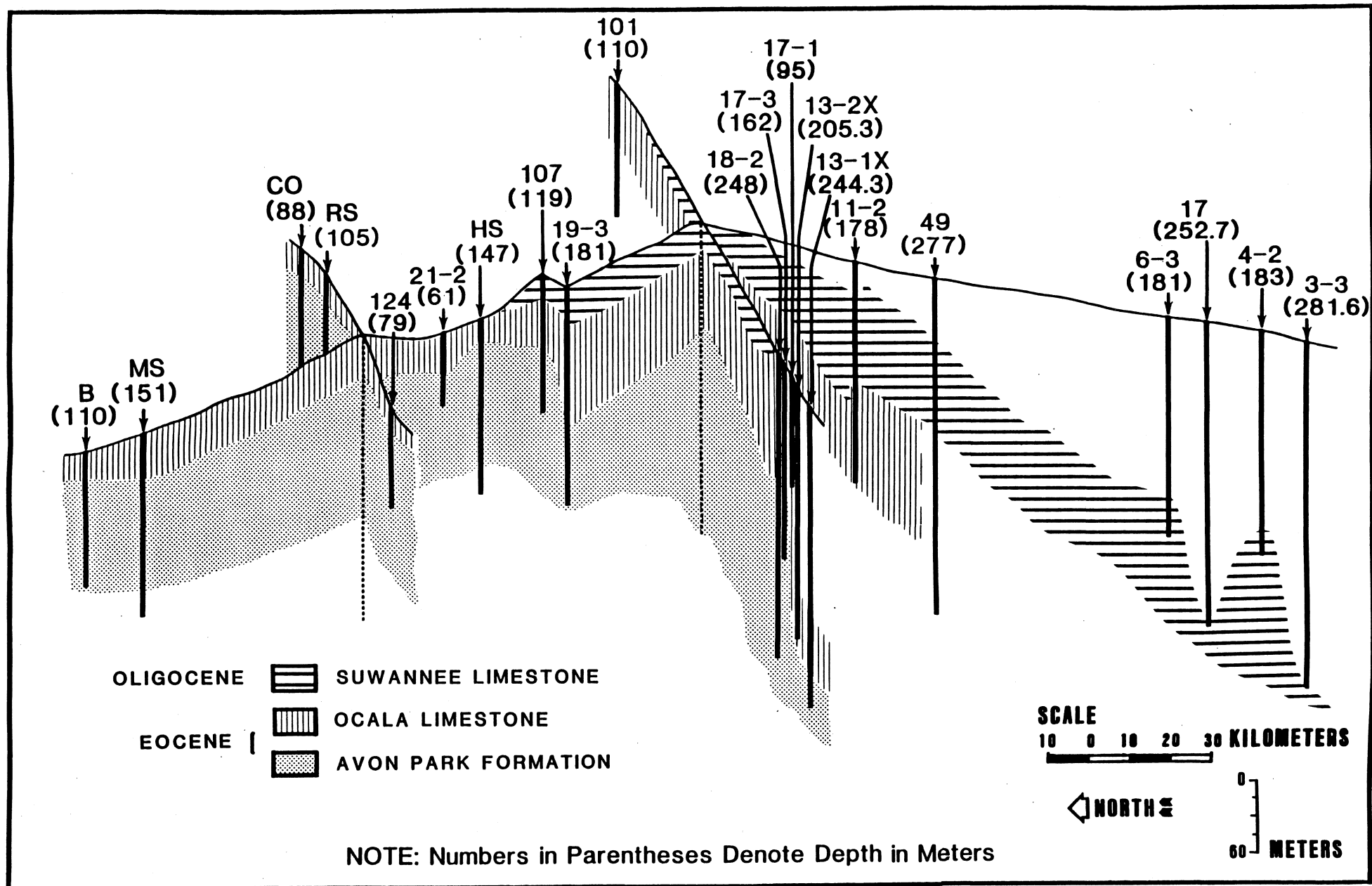
Figure 24. Stratigraphy of the carbonate rocks of the Upper Floridan Aquifer System. Locations for this panel diagram are keyed to Figure 1.

The Avon Park Formation (Applin and Applin, 1944) represents shallow water carbonate deposition with many unconformities denoting subaerial exposure and erosion. This formation generally consists of off-lapping sequences of variably dolomitized, mud-rich carbonates (Randazzo and Saroop, 1976; Randazzo et al., 1977; Randazzo and Hickey, 1978; Fenk, 1979; Sharpe, 1980; Randazzo and Bloom, 1985; Randazzo and Cook 1987; Quinn, 1988). Evaporite mineral deposits are prominent in certain sections, representing tidal flat deposition.

The Ocala Limestone (upper Eocene) overlies the Avon Park Formation (middle Eocene) unconformably. The Ocala becomes progressively more deeper water and open-marine in character up section. This reflects higher sea level stands in the late Eocene. The lower portion of the Ocala is partially dolomitized. Lime mud and biserial foraminifers are more abundant in parts of the upper Ocala indicating decreased water energy and increased water depth (Quinn, 1988).

The Suwannee Limestone (Oligocene) occurs to a more limited extent because of post-Oligocene erosion, associated with a global fall in sea level. The unit is basically limestone but dolomite and quartz sand have been noted as minor constituents of this formation (Randazzo, 1972; Yon and Hendry, 1972; Sharpe, 1980; Miller, 1986). However, only in four of the cores of this study has dolomite been recognized as a dominant mineralogical constituent (Aardema,

1987; Quinn, 1988), at least in certain intervals. The lithofacies present suggest deposition in shallow marine environments with fluctuating sea level conditions. Generally low to moderate energy water circulation occurred but was interrupted by higher-energy currents (Quinn, 1988).

Comparison of figures 22 and 24 reveals a general relationship between stratigraphy and visible porosity type and abundance. This relation is a reflection of the depositional and diagenetic history of each stratigraphic unit. Shallow water deposits, often more fine-grained, were subjected to more numerous changes in diagenetic regimes (migration of the mixing zone). Dissolution and dolomitization played a dominant role in porosity evolution of rocks from such environments. The Avon Park, lower Ocala, and sections of the Suwannee were particularly affected in this way. Deeper water deposits produced rock types reflecting different original porosity and were more limited to the degree and frequency of diagenetic changes related to mixing zones.

Porosity and Lithofacies - Lithofacies relationships are depicted in figures 25-29. These figures show the vertical distribution of faunally dominated rock bodies, within the stratigraphic units. At least seven subfacies are recognized for the Avon Park Formation, ranging from crystalline dolomite to mudstone. Gradational wackestones, packstones, and grainstones also occur. Numerous subfacies are recognized for the Ocala Limestone and the Suwannee
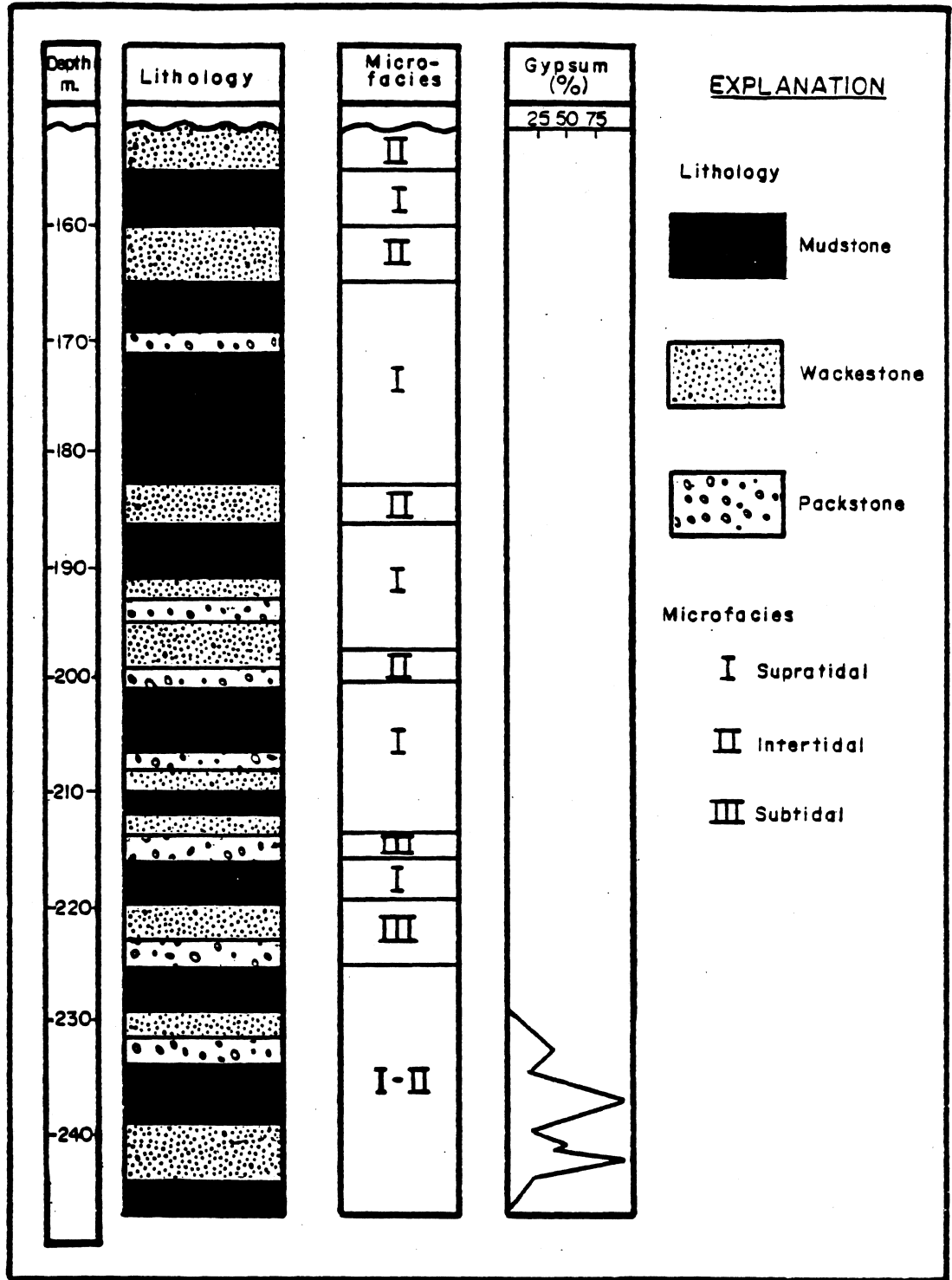
Figure 25. Lithology, microfacies, and evaporite content of core TR 18-2.
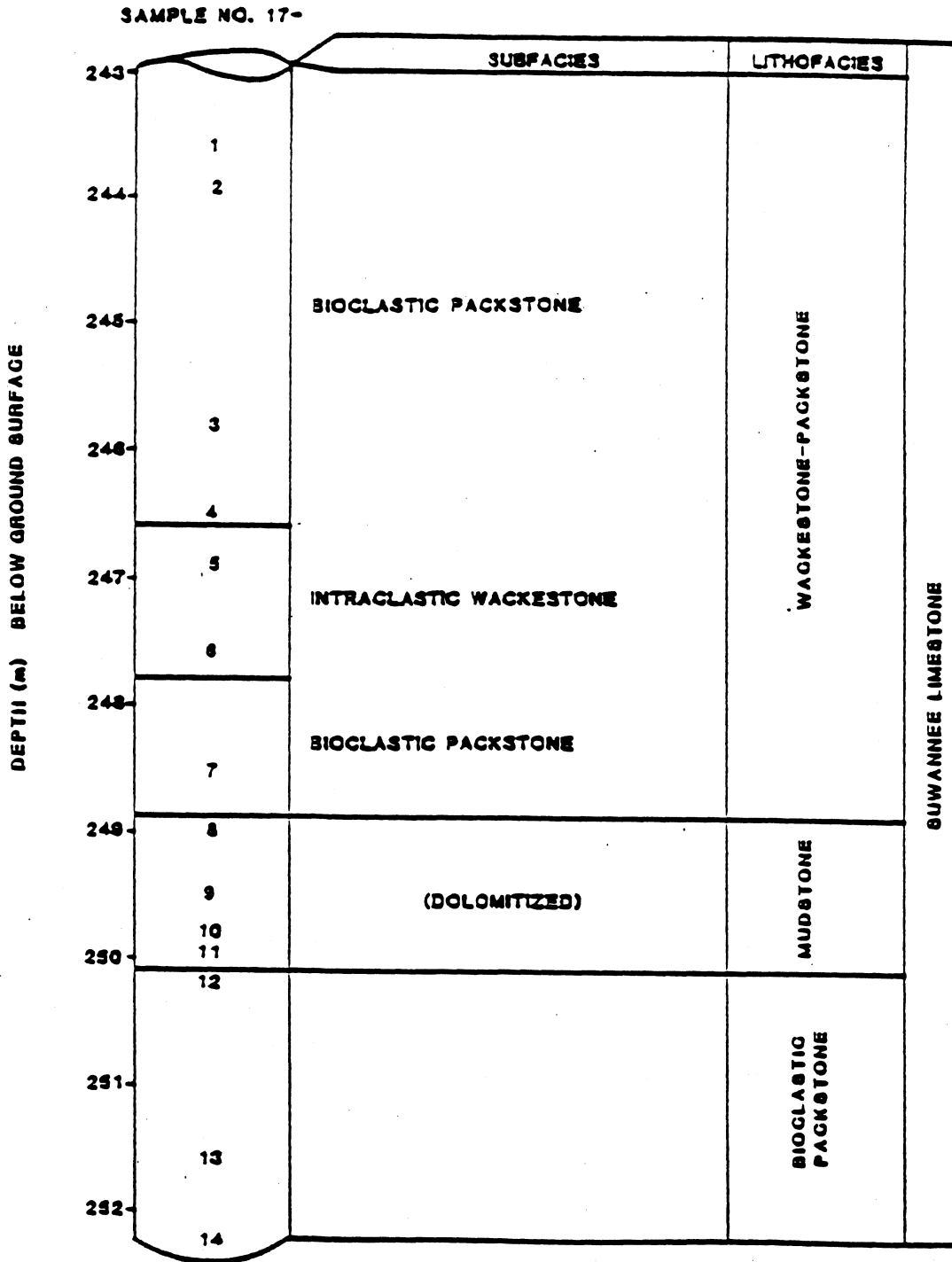
Figure 26. Columnar section of core ROMP 17 showing lithofacies and stratigraphic relationships (after Aardema, 1987).
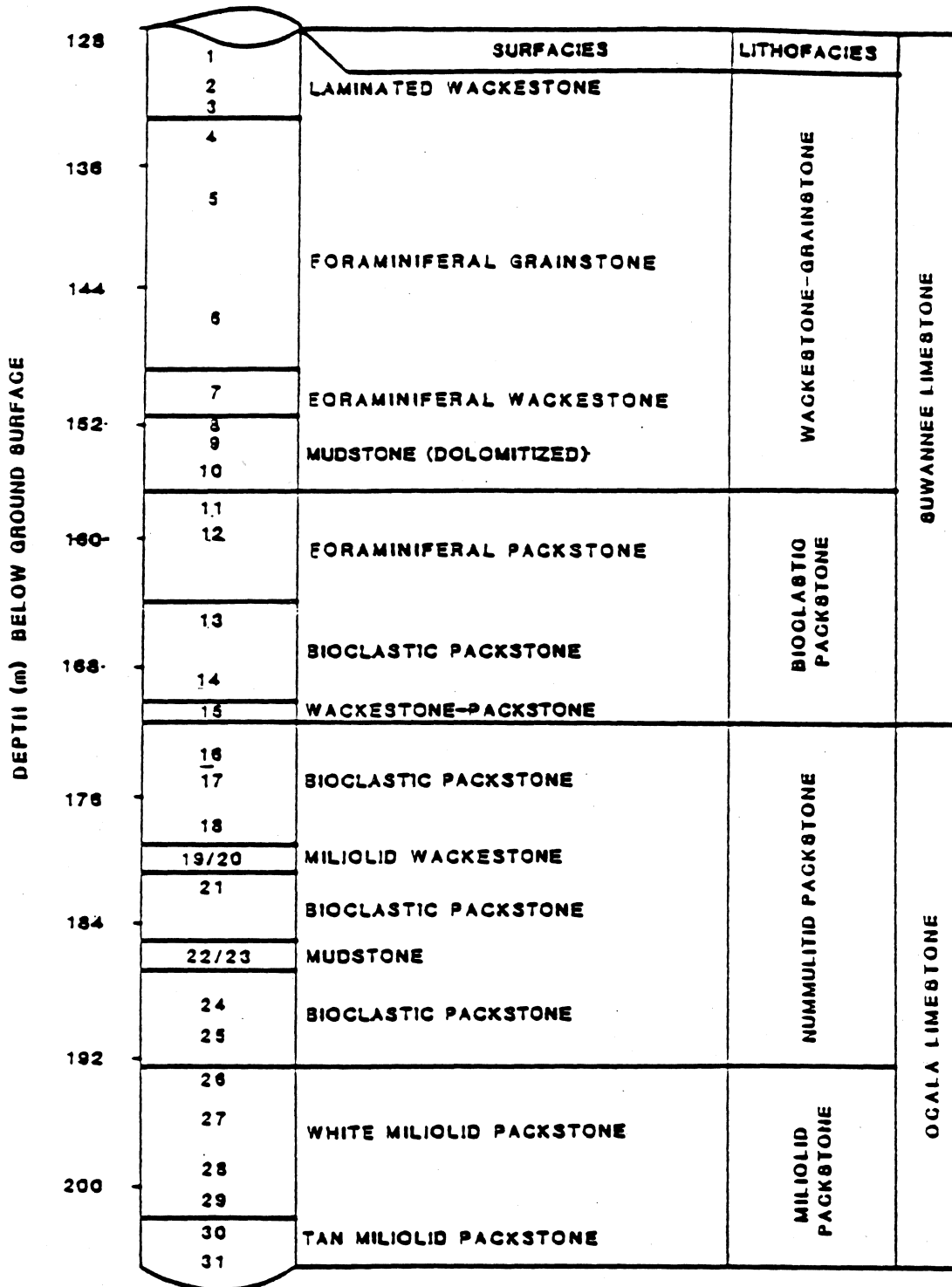
Figure 27. Columnar section of core TR 13-2X showing lithofacies and stratigraphic relationships (after Aardema, 1987).
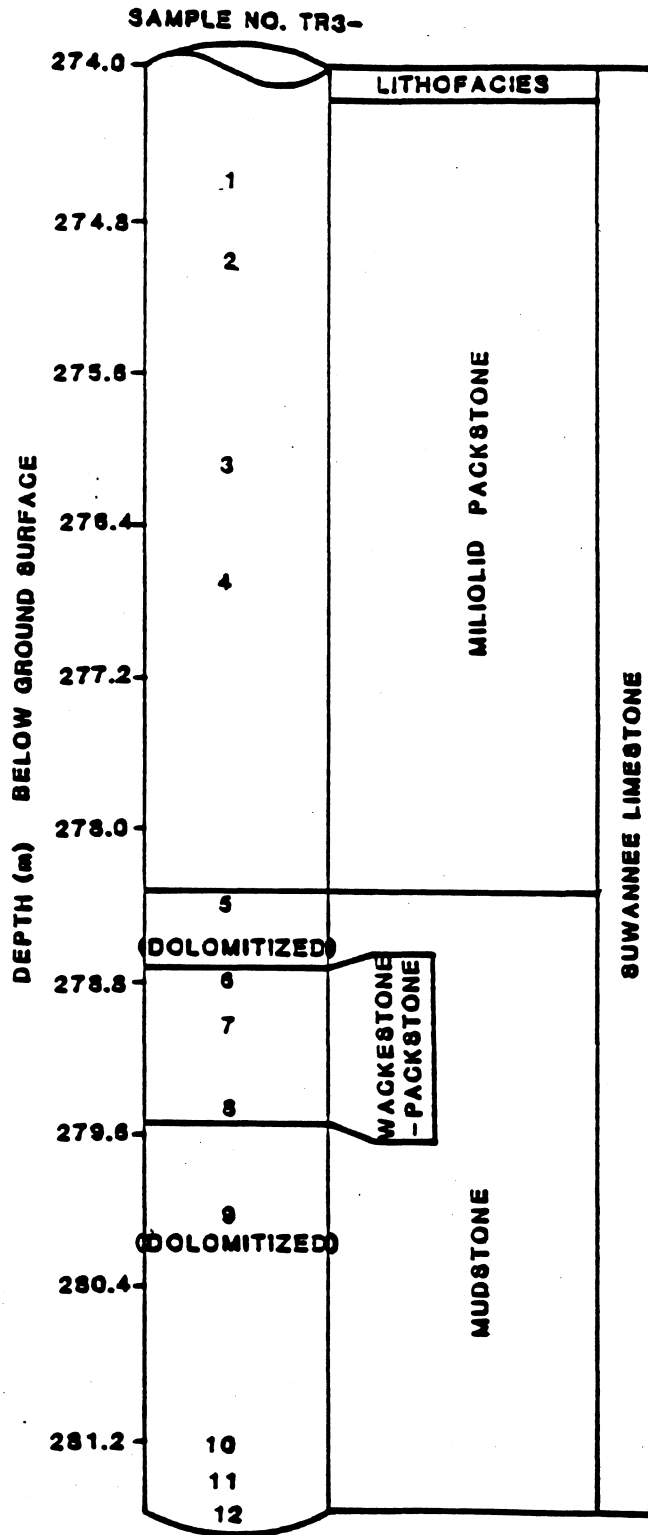
Figure 28. Columnar section of core TR 3-3 showing lithofacies and stratigraphic relationships (after Aardema, 1987).
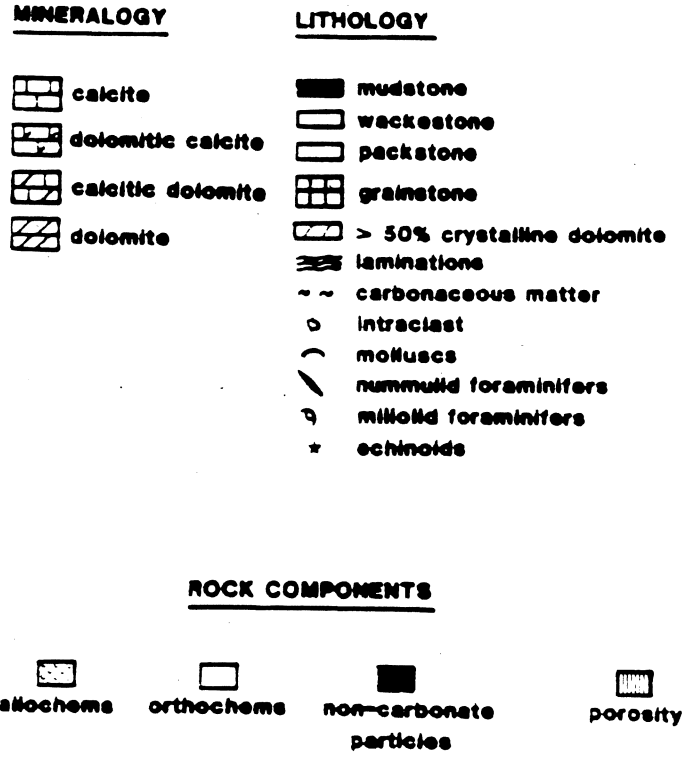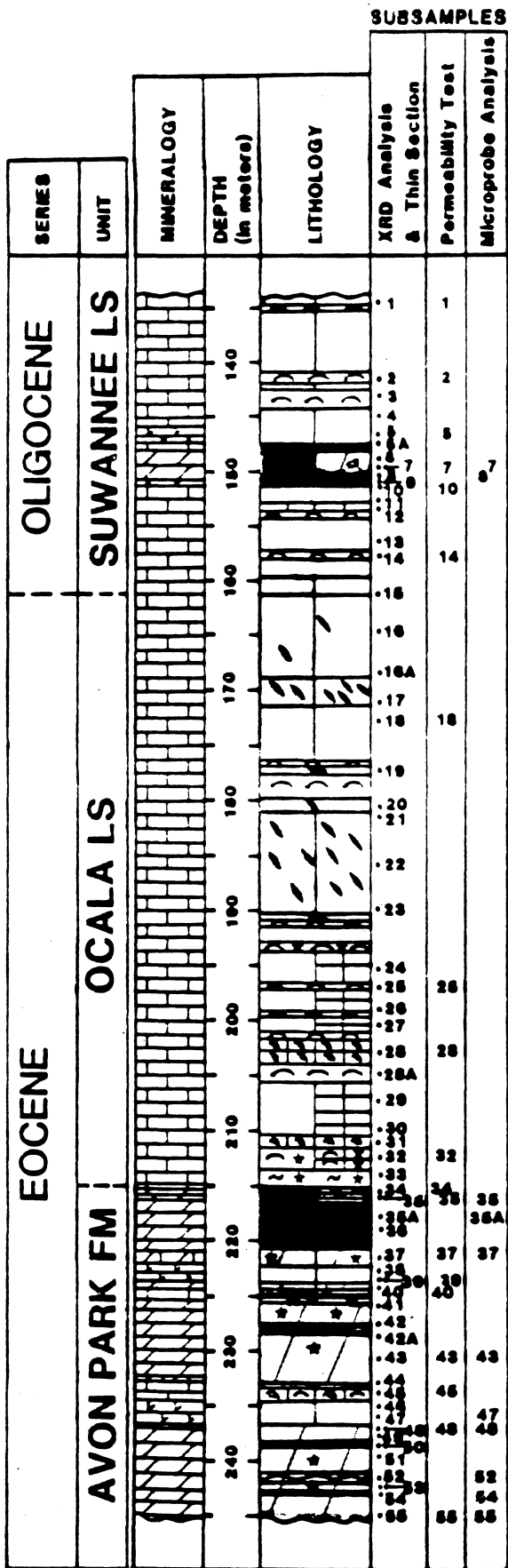
Figure 29. Columnar section of core TR 13-1X showing mineralogy, lithology, stratigraphy, and subsample locations (after Quinn, 1988).

Limestone as well. In general these younger stratigraphic units are composed of more packstone and grainstone facies than the older Avon Park Formation.

Porosity types and occurrences for the cores studied are listed in Table 1. Quinn (1988) graphically compared the lithofacies of core 13-1X directly to vertical variations in porosity (Fig. 29). She demonstrated the relationship of low porosity with mud-rich and dolomitic rocks and greater porosity in nondolomitic, deeper-water deposited limestones. These relationships appear to hold for all three of the stratigraphic units studied. Comparisons of the lithofacies of cores TR18-2X (Fig. 25), ROMP17 (Fig. 26), TR13-2X (Fig. 27), and TR3-3 (Fig. 28) with vertical variations in porosity (Fig. 22) reflect both similar and dissimilar relationships. Generally, nondolomitic, grain-supported grainstones and packstones had greater porosity while nondolomitic mudstones and wackestones had lower porosity. Some dolomite sections had relatively higher porosity, while others had lower.

The distribution of dolomite within the Upper Floridan Aquifer System (Fig. 30) is also related directly to the distributions of porosity types listed in Table 1. Higher porosity overall and more intercrystal, intracrystal, and vug porosity occur in dolomitic rocks. Moldic porosity is more common in nondolomitic rocks. These porosity types and abundance distributions reflect the nature of dolomitization. Subjection of near-shore, finer-grained
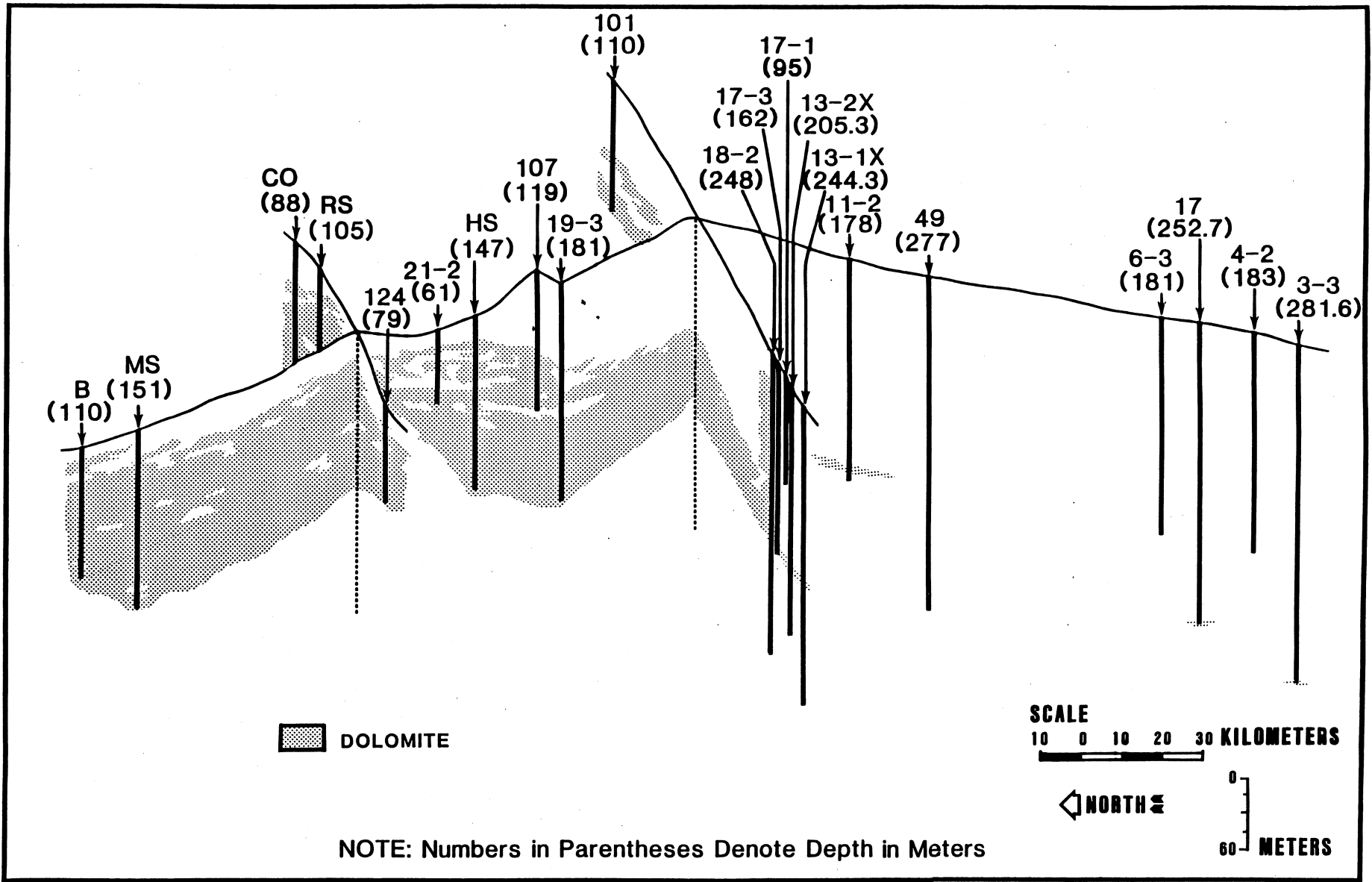
Figure 30. Distribution of dolomite in the carbonate rocks of the Floridan Aquifer System. Locations for this panel diagram are keyed to Figure 1.

carbonate rocks to more frequent groundwater mixing zone
conditions will produce the greatest amount of dissolution
and dolomitization. These important diagenetic processes
will work to enhance and destroy porosity.

Porosity and Trace Elements/Stable Isotopes - The
relationship of porosity to trace element geochemistry and
stable isotope compositions is similar to that recognized
between porosity and dolomite. Figures 31 and 32 show the
general distribution of strontium and sodium in the study
area. They demonstrate higher concentrations of these trace
elements with depth and seaward, the same distribution as
recognized for calcite and dolomite. The trace elements
reflect diagenetic changes in the rocks caused by the same
diagenetic processes responsible for dolomitization. They
support the general understanding of how dolomite has formed
in the Upper Floridan Aquifer System and, therefore, reflect
the same relationship to porosity type and frequency
distributions. Likewise, stable isotope data (carbon and
oxygen) for dolomite (described earlier) also support the
conceptualization of dolomite formation. Isotope data
duplicates the trace element and dolomite relationship to
porosity in the Upper Floridan Aquifer System.

Porosity Formation Today - Present day porosity is the
result of an evolutionary process begun tens of millions of
years ago. It is a reflection of original rock types and
the diagenetic processes acting upon them. The dynamics of
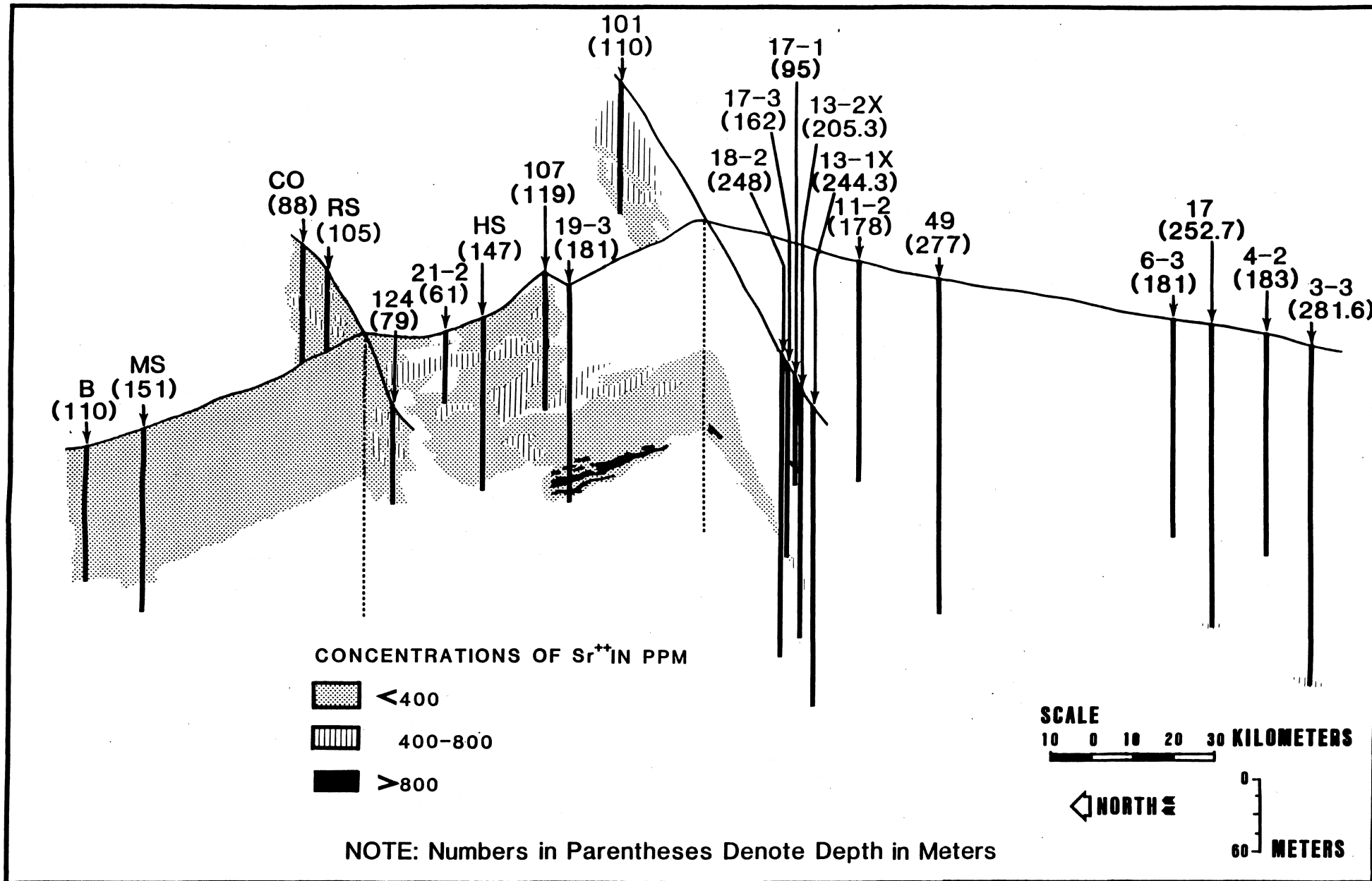
Figure 31.   Distribution of strontium in the carbonate rocks of the Floridan Aquifer System.   Locations for this panel diagram are keyed to Figure 1.
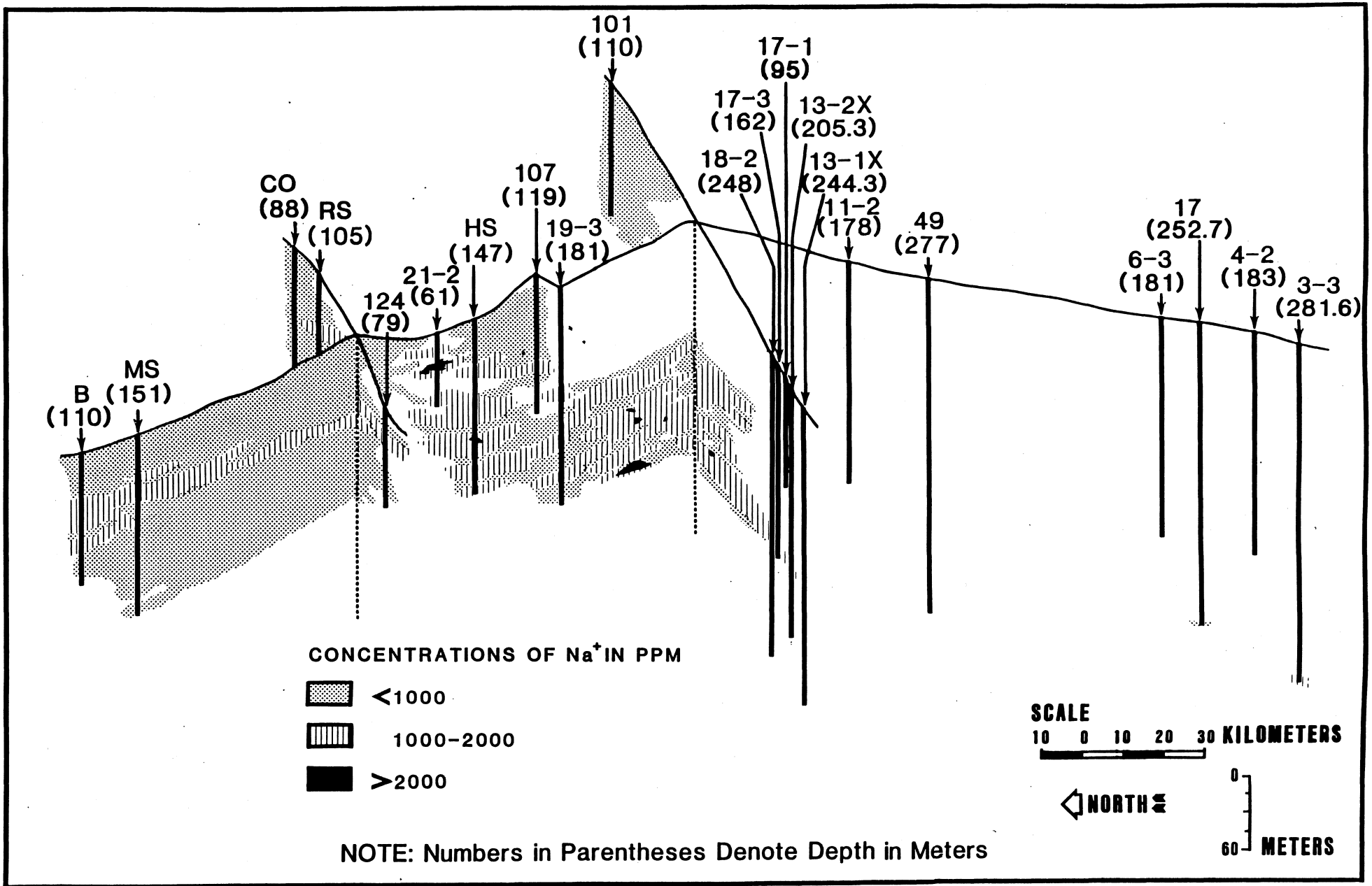
Figure 32. Distribution of sodium in the carbonate rocks of the Floridan Aquifer System. Locations for this panel diagram are keyed to Figure 1.

groundwater flow and the chemical characteristics (both rock and water) of the Upper Floridan Aquifer System have been examined in the context of porosity development. In the coastal area of the SWFWMD, carbonate rocks of this aquifer system are being subjected to several hydrologic flow regimes, principally driven from areas of recharge. These are illustrated in Figure 24. Similarly, these rocks are also subjected to several chemical regimes, principally vadose, freshwater phreatic, brackish transitional (mixing zone) and saline environments.

Conditions favorable for the dissolution of calcite and precipitation of dolomite have been documented by Hanshaw and Back (1979) and Randazzo and Cook (1987), among others. Likewise, certain areas appear to be favorable to calcite precipitation. Complexities of slow kinetics of reactions and the presence of competing ions have altered a rather straight-forward understanding of mineral phase formation or destruction. The nonuniform lithologic characteristics of the aquifer rocks further complicate interpretation and predictions.

The five cores focused upon in this study, when integrated with earlier studies of rocks from the same stratigraphic and hydrologic horizons, illustrate the complexities and variabilities associated with porosity development. Dissolution of dolomite and the creation of intra- and intercrystal porosity and vug porosity is well illustrated in Figures 17 and 18.

Similarly, calcite dissolution and the creation of moldic and vug porosity has also been documented (Figs. 5 and 15). Porosity destruction through dolomite and calcite pore-fillings is commonly observed (Figs. 8 and 11).

The areas of noncavernous porosity development (Fig. 22) will not change appreciably because of the slow rates of mineral dissolution (Brooks, 1969; Sanford, 1987) and formation. Thus, those distributions of porosity type and abundance recognized from this study, when enhanced by future investigations, can be utilized in a modular way to better understand the physical and chemical groundwater conditions. Such an understanding is essential to models addressing transport, pollution, and water inventory questions concerning the Upper Floridan Aquifer System.

ACKNOWLEDGEMENTS

66

data in this report while graduate students under my direction. The information provided in this report must be credited in large part to their dedicated and professional effort to the research accomplished.

Thanks are extended to Jon Jee of the University of Florida for his tireless labor in preparing many of the illustrations and photographs used in this report. Daniel Muller of the Geological Institute, ETH Zentrum, Zurich, Switzerland provided the stable isotope analysis.

REFERENCES CITED

Aardema, J.A., 1987, Petrography and geochemistry of three
     drill cores which penetrate the Suwannee Limestone in
     Pinellas, DeSoto, and Charlotte Counties, Florida
     [unpub. master's thesis]: Gainesville, Univ. of
     Florida, 127 p.

Applin, P.L., and Applin, E.R., 1944, Regional subsurface
     stratigraphy and structure of Florida and southern
     Georgia: American Association Petroleum Geologists
     Bull., v. 28, p. 1673-1753.

Back, W., and Hanshaw, B.B., 1970, Comparison of chemical
     hydrogeology of carbonate peninsulas of Florida and
     Yucatan: Jour. Hydrology, v. 10, p. 330-368.

Back, W., Hanshaw, B.B., Herman, J.S., and Van Driels, J.N.,
     1986, Differential dissolution of a Pleistocene reef in
     the ground-water mixing zone of coastal Yucatan,
     Mexico: Geology, v. 14, p. 137-140.

Bathhurst, R.G.C., 1975, Carbonate Sediments and Their
     Diagenesis (2nd ed.): New York, Elsevier, 658 p.

Blatt, H., Middleton, G., and Murray, R.C., 1980, Origin of
     Sedimentary Rocks (2nd ed.): Englewood Cliffs, New
     Jersey, Prentice-Hall, Inc., 782 p.

Brooks, H.K., 1969, Rate of solution of limestone in the
     Karst terrane of Florida: Florida Water Resources
     Research Center, University of Florida, publication no.
     6, 16 p.

Chen, C.S., 1965, The regional lithostratigraphic analysis
     of Paleocene and Eocene rocks of Florida: Florida
     Geol. Survey Bull., v. 45, 105 p.

Choquette, P.W., and Pray, L.C., 1970, Geologic nomenclature
     and classification of porosity in sedimentary
     carbonates: American Association Petroleum Geologists
     Bull., v. 54, p. 207-250.

Enos, P., and Sawatsky, L.H., 1981, Pore networks in
     Holocene carbonate sediments: Jour. Sedimentary
     Petrology, v. 51, p. 961-985.

Fenk, E.M., 1979, Sedimentology and stratigraphy of middle
     and upper Eocene carbonate rocks, Lake, Hernando, and
     Levy Counties, Florida [unpub. master's thesis]:
     Gainesville, Univ. of Florida, 133 p.

Folk, R.L., 1962, Spectral subdivision of limestones, in Ham, W.E., ed., Classification of Carbonate Rocks: American Association Petroleum Geologists Mem. 1, p. 62-84.

Folk, R.L., and Land, L.S., 1975, Mg/Ca ratio and salinity: Two controls over crystallization of dolomites: American Association Petroleum Geologists Bull., v. 59, p. 60-68.

Friedman, G.M., and Sanders, J.E., 1978, Principles of Sedimentology: New York, John Wiley & Sons, 792 p.

Hanshaw, B.B., and Back, W., 1979, Major chemical processes in the evolution of carbonate-aquifer systems: Jour. Hydrology, v. 42, p. 287-312.

Hanshaw, B.B., Back, W., and Deike, R.G., 1971, A geochemical hypothesis for dolomitization by groundwater: Economic Geology, v. 66, p. 710-724.

James, N.P., and Choquette, P.W., 1984, Limestones -- the meteoric diagenetic environment: Geoscience Canada, v. 7, p. 161-194.

Kobluk, D.R., and Risk, M.H., 1977, Micritization and carbonate-grain binding endolithic algae: American Association Petroleum Geologists Bull., v. 61, p. 1069-1082.

Longman, M.W., 1980, Carbonate diagenetic textures from nearsurface diagenetic environments: American Association Petroleum Geologists Bull., v. 64, p. 461-487.

Miller, J.A., 1986, Hydrogeologic framework of the Floridan aquifer system: U.S. Geol. Survey Prof. Paper 1403-B, 91 p.

Morrow, D.W., 1982, Dolomite -- Part 1: the chemistry of dolomitization and dolomite precipitation: Geoscience Canada, v. 9, p. 5-13.

Murray, R.C., 1960, Origin of porosity in carbonate rocks: Jour. Sed. Petrology, v. 30, p. 59-84.

Murray, R.C., and Pray, L.C., 1965, Dolomitization and limestone diagenesis - an introduction, in Pray, L.C., and Murray, R.C., eds., Dolomitization and Limestone Diagenesis: A Symposium: Society Economic Paleontologists Mineralogists, Spec. Publ. 13, p 1-2.

Plummer, L.N., Jones, B., and Truesdell, A., 1976, WATEQF: A FORTRAN IV version of WATEQ, a computer program for calculating chemical equilibrium of natural waters: U.S. Geol. Survey Water Resources Investigations 76-13, 63 p.

Powers, R.W., 1962, Arabian Upper Jurassic carbonate rocks, in Ham, E.D., ed., Classification of Carbonate Rocks -- A Symposium: American Associate Petroleum Geologists Mem. 1, p. 122-192.

Quinn, H.A., 1988, Characterization of carbonate rocks from the saline zone of the Floridan Aquifer, Pinellas County, Florida [unpub. master's thesis]: Gainesville, Univ. of Florida, 180 p.

Randazzo, A.F., 1983, Mineralogical model of the Floridan aquifer in the Southwest Florida Water Management District: Water Resources Research Center, University of Florida, Office of Water Resources and Technology, U.S. Department of the Interior, Publication n. 68, 48 p.

Randazzo, A.F., and Bloom, J.I., 1985, Mineralogical changes along the freshwater/saltwater interface of a modern aquifer: Sedimentary Geology, v. 43, p. 219-239.

Randazzo, A.F., and Cook, D.J., 1987, Characterization of dolomitic rocks from the coastal mixing zone of the Floridan aquifer, Florida, U.S.A.: Sedimentary Geology, v. 54, p. 169-192.

Randazzo, A.F., and Hickey, E.W., 1978, Dolomitization of the Floridan aquifer: American Jour. Science, v. 278, p. 1177-1184.

Randazzo, A.F., and Saroop, H.C., 1976, Sedimentology and paleoecology of Middle and Upper Eocene carbonate shoreline sequences, Crystal River, Florida, U.S.A.: Sedimentary Geology, v. 15, p. 259-291.

Randazzo, A.F., Sarver, T.J., and Metrin, D.B., 1983, Selected geochemical factors influencing diagenesis of Eocene carbonate rocs, Peninsular Florida, U.S.A.: Sedimentary Geology, v. 36, p. 1-14.

Randazzo, A.F., Stone, G.C., and Saroop, H.C., 1977, Diagenesis of middle and upper Eocene carbonate shoreline sequences, central Florida: American Association Petroleum Geologists Bull., v. 61, p. 492-503.

Randazzo, A.F., and Zachos, L.G., 1984, Classification and description of dolomite fabrics of rocks from the Floridan aquifer U.S.A.: Sedimentary Geology, v. 37, p. 151-162.

Sanford, W.E., 1987, Assessing the potential for calcite dissolution in coastal saltwater mixing zones [unpub. Ph.D. dissertation]: State College, Pennsylvania, Pennsylvania State Univ., 110 p.

Schmoker, J.W., and Halley, R.B., 1982, Carbonate porosity versus depth: a predictable relation for south Florida: American Association Petroleum Geologists Bull., v. 66, p. 2561-2570.

Schmoker, J.W., and Hester, T.C., 1986, Porosity of the Miami Limestone (Late Pleistocene) lower Florida Keys: Jour. Sedimentary Petrology, v. 56, p. 629-634.

Schmoker, J.W., Krystinik, K.B., and Halley, R.B., 1985, Selected characteristics of limestone and dolomite reservoirs in the United States: American Association Petroleum Geologists Bull., v. 69, p. 733-741.

Scholle, P., 1979, Porosity prediction in shallow versus deep water limestone--Primary porosity preservation under burial conditions: American Associate Petroleum Geologists Continuing Education Course Note Series No. 11, section D, p. 1-12.

Sharpe, C.L., 1980, Sedimentological interpretation of Tertiary carbonate rocks from west central Florida [unpub. master's thesis]: Gainesville, Univ. of Florida, 170 p.

Stoessell, R.K., Ward, W.C., Ford, B.H., and Schuffert, J.D., 1989, Water chemistry and $CaCO_3$ dissolution in the saline part of an open-flow mixing zone, coastal Yucatan Peninsula, Mexico: Geol. Soc. America Bull., v. 101, p. 159-169.

Thayer, P.A., and Miller, J.A., 1984, Petrology of lower and middle Eocene carbonate rocks, Floridan aquifer, central Florida: Gulf Coast Association Geol. Societies Transactions, v. 34, 421-434.

Vernon, R.O., 1951, Geology of Citrus and Levy Counties, Florida: Florida Geol. Survey Bull., v. 33, 256 p.

Wardlaw, N.C., 1976, Pore geometry of carbonte rocks as revealed by pore casts and capillary pressure: American Association Petroleum Geologists Bull., v. 60, p. 245-257.

Wolf, K.H., 1965, Grain diminuation of algal colonies to micrite: Jour. Sedimentary Petrology, v. 33, p. 420-427.

Yon, J.W., and Hendry, C.W., 1972, Suwannee Limestone in Hernando and Pasco Counties, Florida: Florida Bureau Geol. Bull., v. 54, part 1, 42 p.